International Journal of Biological Macromolecules 273 (2024) 132968

Contents lists available at ScienceDirect

International Journal of Biological Macromolecules

journal homepage: www.elsevier.com/locate/ijbiomac

Eukaryotic Initiation Translation Factor 2A activation by cannabidiolic acid alters the protein homeostasis balance in glioblastoma cells

Maria Laura Bellone [a], Azmal Ali Syed [b], Rosa Maria Vitale [c], Gianluca Sigismondo [b], Francesca Mensitieri [d], Federica Pollastro [e], Pietro Amodeo [c], Giovanni Appendino [e], Nunziatina De Tommasi [a], Jeroen Krijgsveld [b], Fabrizio Dal Piaz [d,*]

[a] Department of Pharmacy, University of Salerno, Fisciano, Italy
[b] Division of Proteomics of Stem Cells and Cancer, German Cancer Research Center (DKFZ), Heidelberg, Germany
[c] Institute of Biomolecular Chemistry (ICB-CNR), Pozzuoli, Italy
[d] Department of Medicine and Surgery, University of Salerno, Baronissi, Italy
[e] Department of Pharmaceutical Sciences, University of Eastern Piedmont, Vercelli, Italy

ARTICLE INFO

Keywords:
EIF2A
Proteomics
Protein interaction
Ubiquitination
Eukaryotic translation machinery

ABSTRACT

Eukaryotic Initiation Translation Factor 2A (EIF2A) is considered to be primarily responsible for the initiation of translation when a cell is subjected to stressful conditions. However, information regarding this protein is still incomplete. Using a combination of proteomic approaches, we demonstrated that EIF2A is the molecular target of the naturally occurring bioactive compound cannabidiolic acid (CBDA) within human glioblastoma cells. This finding allowed us to undertake a study aimed at obtaining further information on the functions that EIF2A plays in tumor cells. Indeed, our data showed that CBDA is able to activate EIF2A when the cells are in no-stress conditions. It induces conformational changes in the protein structure, thus increasing EIF2A affinity towards the proteins participating in the Eukaryotic Translation Machinery. Consequently, following glioblastoma cells incubation with CBDA we observed an enhanced neosynthesis of proteins involved in the stress response, nucleic acid translation and organization, and protein catabolism. These changes in gene expression resulted in increased levels of ubiquitinated proteins and accumulation of the autophagosome. Our results, in addition to shedding light on the molecular mechanism underlying the biological effect of a phytocannabinoid in cancer cells, demonstrated that EIF2A plays a critical role in regulation of protein homeostasis.

1. Introduction

Investigating the role played by a protein in the cellular context is quite challenging, especially because such a study should be conducted by limiting perturbations to the system as much as possible. Indeed, experimental approaches such as silencing or mutation of a gene result in numerous changes in the cells studied, thus making it difficult to understand which of these depend directly on the lack of activity of a protein and which instead on the adaptation of the biological system to that lack [1,2]. In the last years, the use of small molecules as a tool to shed-light on protein functions under pseudo-physiological conditions is emerging forcefully [3,4]. This approach is generally conducted using specific modulators for a predetermined target [5,6]. However, applying this procedure in a non-targeted manner could also allow characterizing proteins that, despite playing a critical role in both cellular physiology and specific pathological conditions, have so far been little studied.

In this context, phytocannabinoids could represent rather promising candidates. They are the bioactive constituents of *Cannabis sativa* L. [7], showing a wide panel of biological activities. Preparations based on *C. sativa* extracts are currently employed to treat several diseases and severe pain, and to reduce the undesirable effects of antineoplastic therapies [8,9]. Unfortunately, the knowledge of the complex profile of biological targets of these compounds is still inadequate. In fact, even the activity of the best-known phytocannabinoids - Δ^9-tetrahydrocannabinol (Δ^9-THC) and cannabidiol (CBD) - has only been partially characterized [10–14]. This criticality is made even more severe by the lack of information regarding the bioactivity of the other phytocannabinoids. One of the major areas of mechanistic and clinical uncertainty on the potential of cannabis is cancer [15]. Although the ability to activate Endoplasmic Reticulum (ER) stress [16] has been suggested as

* Corresponding author.
E-mail address: fdalpiaz@unisa.it (F. Dal Piaz).

https://doi.org/10.1016/j.ijbiomac.2024.132968
Received 4 March 2024; Received in revised form 1 June 2024; Accepted 5 June 2024
Available online 11 June 2024

the base for the pro-apoptotic and pro-autophagic properties of phytocannabinoids in several cancer cell line [12,17–19], the picture is largely unclear.

One of the most abundant but less investigated phytocannabinoids, is the cannabidioic acid (CBDA) (Fig. 1). It is the main native constituent of fibrous cannabis and its concentration in many preparations based on cannabis extracts is almost comparable to that of CBD [7,20]. It is credited for anti-inflammatory [21], anti-proliferative [22] antibiotic [23], antioxidant activities [24] and is characterized by an excellent ability to cross the Blood-Brain-Barrier [25]. Nevertheless, its molecular targets are still substantially unknown. Indeed, it has been shown that CBDA has only modest/moderate affinity towards CB receptors, 5-HT1A and TRP channels [26], and nuclear receptors belonging to the PPAR family have been suggested as its putative targets [27–29]. Based on these considerations, we chose to use cannabidioic acid (CBDA) as a probe to identify potentially druggable proteins within human tumor cells and to characterize their functions. Thus, we used an integrated approach consisting of proteomic, biochemical and computational techniques [30], to identify the molecular targets of CBDA in a glioblastoma cell line. The obtained results showed that the phytocannabinoid efficiently interacts with Eukaryotic Initiation Factor 2A (EIF2A). Therefore, we investigated the CBDA-EIF2A binding in molecular detail and the cannabinoid-induced changes in the interactome and in the activity of EIF2A in its cell environment. Furthermore, our outputs indicated that EIF2A plays a pivotal role in regulating protein homeostasis by activating the ubiquitination process and the autophagosome formation.

2. Methods

2.1. Reagents and materials

CBDA was purified starting from plant material, while cannabichromenic acid (CBCA) was obtained by synthesis (see below). Silica gel 60 (70–230 mesh), RP C-18 silica gel and Celite® 545 particle size 0.02–0.1 mm, pH 10 (100 g/L, H2O, 20 °C), used for isolation of cannabinoids, was purchased from Macherey-Nagel (Düren, Germany). Purifications were monitored by TLC on Merck 60 F254 (0.25 mm) plates and visualized by staining with 5 % H_2SO_4 in EtOH and overheating. Identification and purity of CBDA and CBCA was 99.9 % as proved by HPLC and ^{1}H NMR 400 MHz analyses with Bruker 400 spectrometers (Bruker®, Billerica, MA, USA). Chemical shifts were referenced to the residual solvent signal (CDCl3: δH = 7.26). The purity of all compounds was 99.9 % as proved by HPLC and NMR analyses. Each compound was dissolved in DMSO at a concentration of 50 mM to obtain a stock solution. ([3-(4,5-dimethylthiazol-2-yl)-2,5-diphenyl tetrazolium bromide]) MTT was purchased from Sigma-Aldrich (St. Louis, Missouri, United States). Click-IT Protein Enrichment Kit, Dulbecco Eagles's medium (DMEM), Dulbecco's Phosphate Buffered Saline (PBS), 0.5 % Trypsin-EDTA, dialyzed fetal bovine serum (FBS), BCA Protein Assay Kit and Corning Matrigel were purchased from Thermo Fisher Scientific (Waltham, Massachusetts, United States). DMEM-High Glucose for the preparation of SILAC medium was purchased from Athena Enzyme Systems (Baltimore, United States). EIF2A primary antibody for immunoprecipitation and immunoblotting were purchased from Proteintech (Rosemont, Illinois). pEIF2α and LC3I/II were purchased from Cell Signaling (Danvers, Massachusetts). EIF2α primary

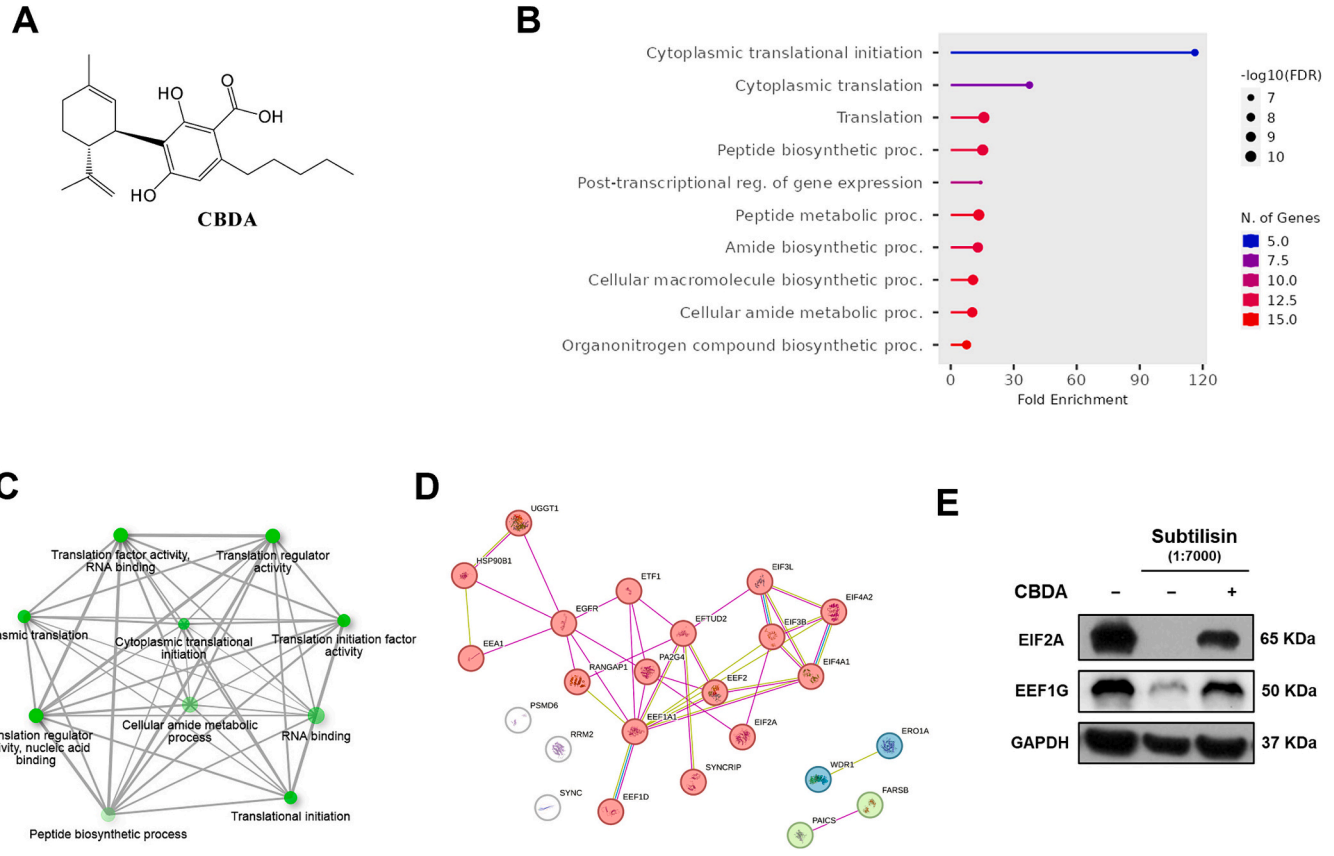

Fig. 1. Identification of CBDA putative target in U87MG cells A) Chemical structure of cannabidiolic acid (CBDA); B) Biological functions of the proteins emerged as putative CBDA targets form DARTS analysis, clusterized by ShinyGO 0.8 software; C) Network of the biological functions of the proteins identified as putative CBDA targets; D) Network of the physical interactions occurring between the proteins emerged as putative CBDA targets form DARTS analysis; E) Western blot analysis of DARTS experiment carried out on U87MG treated with CBDA, using anti-EIF2A and anti-EEF1G antibodies. GAPDH was used as a control;

antibodies was purchased from ElabScience (Houston, Texas). GRP78 primary antibody was purchased from Invitrogen (Waltham, Massachusetts). Mono-and poly-ubiquitinylated conjugates antibody was purchased from Enzo Life Sciences. Anti-SQSTM1 / p62 antibody was purchased from Abcam (Cambridge, United Kingdom). Protein A/G PLUS Agarose and EEF1G primary antibody were purchased from SantaCruz Biotechnology (Dallas, Texas, United States). Secondary antibodies were purchased from Jackson ImmunoResearch Laboratories (West Grove, Pennsylvania). For pulsed-SILAC, labeling amino acids, $^{13}C_6^{14}N_4$-L-arginine (Arg6), 4,4,5,5-D_4-L-lysine (Lys4), $^{13}C_6^{15}N_4$-L-arginine (Arg10) and $^{13}C_6^{15}N_2$-L-Lysine (Lys8) were purchased from Silantes (Gollierstraße, München, Germany). For the peptide clean-up, Oasis plates were purchased from Waters Corporation (Milford, Massachusetts, United States). For SPR analysis, EIF2A recombinant protein was purchased by BIOTREND Chemicals, LLC (Miramar Beach, United States). EEF1G was purchased by OriGene Global (Rockville, United States). HBS-EP 10× buffer and CM5 sensor chip were purchased by GE Healthcare (Chicago, IL, United States).

2.2. Cannabinoid isolation and characterization

CBDA was isolated from *Cannabis sativa* L. (voucher specimen LANZHOU-84/2019) aerial parts (100 g), which were extracted with acetone (2 × 1 L) in a vertical percolator at room temperature, to afford a dark doughty liquid. The resulting latter latex was dissolved at 45 °C in MeOH (with a latex/MeOH ratio 1:10 *w/v*) and kept at 8 °C to facilitate the condensation of fatty material and waxes. After 12 h, the solution was vacuum-filtered with cold MeOH in a sintered funnel protected by a bed of stratified Celite® and finally evaporated at reduced pressure. The fraction obtained after evaporation was subsequently vacuum filtered by solid-phase extraction on RP C-18 silica gel to remove pigments, unsaturated fatty acids, and poly-isoprenoids. For this purpose, the fraction was dissolved in the minimal MeOH amount at 45 °C and charged on RP C-18 (with a ratio raw fraction/stationary phase 1:5 *w*/w), packed with MeOH in a sintered funnel (9 × 15 cm) with a side arm for vacuum. Elution with MeOH (100 mL) gave a purified fraction. The de-fatty extract was dissolved in 50 mL of petroleum ether and 5 mL of acetone in a separating funnel and partitioned twice with 100 mL of NaOH 2 % in H_2O. The basic solution containing the natrium salt of cannabinoid acids was then acidified to pH = 3 with H_2SO_4 until the formation of a milky mixture. This latter acidified fraction was then partitioned with CH_2Cl_2 (2 × 50 mL), anhydrified with Na_2SO_4, and evaporated affording a fraction containing raw cannabinoid acids.

The cannabinoid acids fraction was purified by low-pressure chromatography (LPC) on silica gel (with a ratio raw fraction/stationary phase 1:50 *w*/w, petroleum ether-EtOAc gradient from 80:20 to 60:40 *v*/v) to afford the purified cannabinoid acids. Following the procedure, 1.49 g of CBDA [31] were isolated. The phytocannabinoid was identified by ^{1}H NMR, 400 MHz (Fig. S1A) according to the literature data.

To a stirred solution of ethyl olivetolate (500 mg, 1.982 mmol, 1.04 eq) in toluene (10 mL), citrale (327 L, 1.905 mmol, 1 eq) and n-butylamine (188 L, 1.905 mmol, 1 eq) were sequentially added. The mixture was refluxed overnight, then quenched with 2 M H_2SO_4 (50 mL) and extracted with ethyl acetate (3 × 50 mL). The combined organic phases were washed with BRINE, dried over Na_2SO_4 and evaporated. The resulting crude was then dissolved in KOH 3 M (solution in MeOH/H_2O 1:1, 10 mL) and heated to 40 °C for 4 days. The reaction was then quenched with H_2SO_4 2 M (50 mL) and extracted with ethyl acetate (3 × 50 mL). The combined organic phases were washed with BRINE, dried over Na_2SO_4 and evaporated. Purification over silica gel (PE:EtOAc 9:1 as eluent) afforded 145 mg of brown oil (20 % yield) identified as pure CBCA 4 by ^{1}H NMR, 400 MHz according to the literature data [32] (Fig. S1B).

2.3. Cell culture

Human glioma cells (U87MG) (ECACC No: 89081402) were grown in DMEM supplemented with 1 % penicillin/streptomycin, 1 % L-glutamine, 1 % sodium pyruvate, 1 % non-essential amino acids and 10 % FBS. Cells were maintained under a humidified atmosphere with 5 % CO_2 at 37 °C. Normal human astrocytes (NHA) were grown in AGM™ BulletKit™ (CC-3186). Cells were maintained under a humidified atmosphere with 5 % CO2 at 37 °C.

2.4. Cellular viability assay

Cell viability was measured by MTT assay (Sigma). U87MG and NHA cells were seeded at $7*10^3$ per well into 96-well plates. The day after, cells were treated with 0.1 % (*v*/v) DMSO or CBDA using cannabinoid concentrations in the range of 25–200 μM. To assess properly the cytotoxic effect, an incubation time of 48 h was selected. Subsequently, the cells were incubated with MTT solution at the final concentration of 1 mg/mL and incubated for 4 h. Then, the resulting MTT-formazan crystals were solubilized in DMSO and the absorbance of the solution at 550 and 620 nm was measured using a Multiskan GO (Thermo Fisher Scientific). Experiments were performed twice and analyzed in three technical replicates. Differences between treatment group and control were analyzed by Student's *t*-test and were considered significant when $p \leq 0.1$ (*) or $p < 0.05$ (**).

2.5. Drug affinity target stability assay (DARTS)

DARTS assay was performed on U87MG and NHA intact cells. U87MG cells were seeded $2*10^5$ per well into 6-well plates in 10 % FBS-DMEM while NHA cells were seeded $6.0*10^4$ per well in 12-well plates. The day after, the cells were treated with 50 μM CBDA, CBCA or 0.1 % (*v*/v) DMSO for 4 h. The cells were lysed in RIPA buffer (20 mM Tris HCl pH 7.5, 150 mM NaCl, 1 mM EDTA, 1 % NP-40, 1 % sodium deoxycholate, 2.5 mM sodium pyrophosphate, 1 mM Na_3VO_4), centrifuged at 14000 rpm for 20 min. Then, 50 μg of protein lysate were subjected to a limited digestion with subtilisin (enzyme:protein 1:3500 and 1:7000 *w*/w) for 30 min at 37 °C. DARTS on U87MG cell lysate was performed first by lysing the untreated cells in RIPA buffer as described above. Then, 100 μg of cell lysate were treated with 50 μM CBDA or 0.1 % (*v*/v) DMSO, for 1 h on ice. The protein lysates were subjected to a limited digestion with subtilisin (enzyme:protein 1:7000 *w*/w) for 30 min at 37 °C. The reactions of both DARTS approaches were stopped by adding Laemmli buffer 4× and incubating the mixture at 95 °C for 5 min. The samples underwent electrophoretic separation by SDS-PAGE. The obtained gels were divided into 10 pieces and digested as reported elsewhere [33]. Mass spectrometry analysis of the tryptic peptides was performed using Q-Exactive Orbitrap instrument (Thermo Fisher Scientific), coupled with a nanoUltimate3000 UHPLC system (Thermo Fisher Scientific). Peptide separation was performed on a capillary EASY-Spray PepMap column (0.075 mm × 50 mm, 2 μm, Thermo Fisher Scientific) using aqueous 0.1 % formic acid (A) and CH_3CN containing 0.1 % formic acid (B) as mobile phases and a linear gradient from 3 % to 40 % of B in 45 min and a 300 nL/min flow rate. Mass spectra were acquired over a *m/z* range from 375 to 1500. MS and MS/MS data underwent Mascot software (v2.5, Matrix Science, Boston, MA, USA) analysis using the non-redundant data bank UniprotKB/Swiss-Prot. Parameter were set as follows: trypsin cleavage; carbamidomethylation of cysteine as a fixed modification and methionine oxidation as a variable modification; a maximum of two missed cleavages; false discovery rate (FDR), calculated by searching the decoy database, 0.05.

DARTS experiments on intact cells and protein extracts were performed in biological duplicates. Were considered as putative targets only those proteins identified in the treated samples and not in the control ones in all the measurements. The analysis of protein functions was performed using the gene ontology tool in the UniProt

Knowledgebase (UniProtKB; http://www.uniprot.org). Once the putative target protein was identified, western blot was performed under the same experimental condition as before. Densitometric analyses of the resulting bands were carried out using the ImageJ software. GAPDH was used as a normalizer. The experiments were performed three times and the obtained results were compared.

2.6. Cellular thermal shift assay

CETSA assay was performed on a U87MG cell line. The cells were seeded $1*10^5$ per well into 12-well plates in 10 % FBS-DMEM. The day after, the cells were treated with 50 μM CBDA or CBCA or 0.1 % (*v*/v) DMSO for 4 h. After washing, the cells were collected, dissolved in PBS, divided in 12 aliquots each subjected to a 5 min incubation at different temperatures between 53 and 60 °C. Subsequently, the cells were lysed by freeze/thaw cycles and centrifuged. The soluble proteins were separated by a 12 % SDS-PAGE and western blot analysis was carried out. Densitometric analyses of the resulting bands were carried out using the ImageJ software. Glyceraldehyde 3-phosphate dehydrogenase (GAPDH) was used as a normalizer. The experiments were performed three times and the obtained results were compared.

2.7. Surface plasmon resonance

A Biacore 3000 optical biosensor (GE Healthcare, Chicago, IL, USA) was used to perform Surface Plasmon Resonance (SPR) measurements. EIF2A and EEF1G were dissolved in 10 mM sodium acetate, respectively, at pH 6.0 and pH 7.0, and injected on a research-grade CM5 sensor chip at a flow rate of 3 μL/min to achieve immobilization, using a standard amino-coupling protocol. CBDA and CBCA stock solutions were diluted in HBS-EP buffer (0.1 M HEPES, 1.5 M NaCl, 0.03 M EDTA and 0.5 % *v*/v Surfactant P20) to produce a three-concentration points series (1, 5 and 20 μM). All the produced samples contained 0.04 % (*v*/v) DMSO. Measurements were performed at 25 °C, using a 10 μL/min flow rate and adopting an association time of 120 s; dissociation of the complex was monitored for 180 s. The resulting sensorgrams were elaborated by the BIAevaluation software (GE Healthcare). Thermodynamic constants were calculated by adequately fitting the experimental curves with a single-site bimolecular interaction model. The experiments were performed three times and the obtained results were compared.

2.8. Limited proteolysis

To perform Limited proteolysis experiments coupled with MS, U87MG cells were seeded $2*10^5$ per well into 6-well plates in 10 % FBS-DMEM. The day after, the cells were treated with 50 μM CBDA or 0.1 % (*v*/v) DMSO for 4 h. Subsequently, the cells were subjected to not-denaturing lysis and the resulting protein mixtures underwent subtilisin digestion, as previously described for DARTS experiments. Subtilisin was inactivated boiling for 5 min at 95 °C. Then, the cysteine residues were reduced by adding 10 mM dithiothreitol for 30 min at 37 °C and subsequently alkylated by adding 30 mM iodoacetamide for 45 min at room temperature. Once reestablished pH 7.5, proteins were subjected to trypsin/LysC catalyzed digestion, using a 1:100 enzyme/substrate ratio (*w*/w) and an overnight incubation at 37 °C. Sodium deoxycholate was precipitated by adding formic acid to a final concentration of 2 % (*v*/v). Once the final pH of the sample was verified to be <3, purification of the peptide was performed using OasisPlate. The chromatography mini-columns were washed and activated using 1 % formic acid (buffer A) and 60 % methanol with 1 % formic acid (buffer B). Peptide cleaning was carried out using buffer A while their elution was achieved using buffer B. Samples were dried in speed-vac, dissolved in 0.1 % trifluoroacetic acid (TFA) and injected in the mass spectrometer. The mass spectrometry analyses were performed using Tri-Hybrid Orbitrap Fusion mass spectrometer (Thermo Fisher Scientific), coupled with a Easy nLC 1200 nanospray ion source (Thermo Fisher Scientific). Peptides were loaded on a trap column (PepMap100 C18 Nano-Trap 100 μm × 20 mm) and separated over a 25 cm analytical column (Waters nanoEase BEH, 75 μm × 250 mm, C18, 1.7 μm, 130 Å) using aqueous 0.1 % formic acid (A) and 80 % CH_3CN containing 0.1 % formic acid (B) as mobile phases and a linear gradient from 3 % to 100 % of B in 105 min and a 300 nL/min flow rate. Mass spectra were acquired over an *m/z* range from 375 to 1500. MS and MS/MS data underwent MaxQuant software (v2.5, Matrix Science, Boston, MA, USA) analysis using the non-redundant data bank UniprotKB/Swiss-Prot. The experiments were performed three times and the obtained results were compared.

2.9. Computational methods

The three-dimensional model of the full EIF2A was retrieved from AlphaFold Protein Structure Database (https://alphafold.ebi.ac.uk). The protein model underwent energy minimization (EM) and molecular dynamics (MD) simulations with Amber20 pmemd.cuda module, using ff14SB version of Amber force field [34]. To perform MD simulations in solvent, the protein was confined in a TIP3P water periodic box exhibiting a minimum distance between solute atoms and box surfaces of 10 Å, using the tleap module of the AmberTools20 package. The systems were then neutralized by addition of counterions (Cl^-) and subjected to 1000 steps of EM with solute atoms harmonically restrained to their starting positions (Kr = 10 kcal.mol-1.Å-1). Then, a 500 ps restrained MD simulation (Kr = 5 kcal kcal.mol-1.Å-1) at constant pressure (1 atm) was run on the solvated protein, gradually heating the system to 300 K, followed by a 500 ps restrained MD simulation (Kr = 5 kcal.mol-1.Å-1) at constant temperature (300*K*) and pressure (1 atm) to adjust system density. Production MD simulations were carried out at constant temperature (300 K) and pressure (1 atm) for 400 ns, with a time step of 2 fs. Bonds involving hydrogens were constrained using the SHAKE algorithm. Additional 100 ns of MD simulation for the protein alone was carried out to evaluate the relative motion of α-helix 481–495 respect to the stretch 463–472 in comparison to that of CBDA-EIF2A complex. Starting ligands geometry were built with UCSF Chimera program [35], followed by initial EM at AM1 semi-empirical level. The molecules were then fully optimized using the GAMESS program [36] at the Hartree–Fock level with the STO-3G basis set and subjected to HF/6-31G*/STO-3G single-point calculations to derive the partial atomic charges using the RESP procedure [37]. Docking studies were performed with AutoDock 4.2. Both proteins and ligands were processed with AutoDock Tools (ADT) package version 1.5.6rc1 [38] to merge non-polar hydrogens and calculate Gasteiger charges. Grids for docking evaluation with a spacing of 0.375 Å, centered on the protein sites 1–3, were generated using the program AutoGrid 4.2 included in the Autodock 4.2 distribution. The Lamarckian genetic algorithm was adopted to perform 100 docking runs with the following parameters: 100 individuals in a population with a maximum of 15 million energy evaluations and a maximum of 37.000 generations, followed by 300 iterations of Solis and Wets local search. The complexes, selected based on binding energy and cluster population, were completed by addition of all hydrogen atoms, and they underwent EM and MD simulations with Amber20 pmemd.cuda module, using the ff14SB version of the AMBER force field for the protein and gaff parameters for the ligand. The protocol was the same used for the protein alone. Production MD simulations were carried out at constant temperature (300 K) and pressure (1 atm) for 200 ns, with a time step of 2 fs. In MD with distance restraints protocol, time dependent distance restraints were applied over 100 ns MD (from 15 to 4.5 Å) between the center of mass of the 460–480 Cα atoms and the carbon atom of the resorcinol moiety connected to the terpenoid ring, followed by 100 ns of unrestrained MD production run. The cpptraj module of AmberTools20 and program UCSF Chimera 1.10.1 were used to perform MD analysis and to draw the figures, respectively. Cluster analysis was carried out with the cpptraj module using the dbscan clustering algorithm. The representative frames were taken from the most populated clusters of each MD simulation.

2.10. Co-immunoprecipitation experiments

EIF2A co-immunoprecipitation assay was performed using U87MG cells. Cells were seeded $2*10^5$ per well in 6-well plates in 10 % FBS-DMEM. The next day, cells were treated with 50 μM CBDA or 0.1 % (*v*/v) DMSO for 4 h. The cells were lysed in RIPA buffer and centrifuged. The resulting proteins were incubated with the primary anti-EIF2A antibody for 2 h on the rotator (antibody:protein ratio 1:100). Then, the Protein A/G PLUS agarose beads were incubated overnight according to the manufacturer's instructions. Subsequently, the beads were washed gently with a wash buffer, centrifuged at 2000 *g* for 3 min at 4 °C and the supernatants were discarded. After repeating the washing step twice, the proteins were eluted by heating the bead pellet in a 2× SDS loading buffer without DTT for 10 min at 50 °C, which was then centrifuged, and the obtained supernatants collected. Then, a second elution step was performed by heating the beads again in a 2xSDS buffer with 100 mM DTT. The obtained solutions were collected and separated by a 12 % SDS-PAGE. Each lane of the resulting gel was divided into 10 pieces and in-gel digestion followed by MS analyzes were performed, as described in the DARTS paragraph. Finally, protein characterization and quantification were performed using the Proteome Discoverer software by setting the abundance ratio of the CBDA sample to the DMSO control. Proteins identified based on a single unique peptide were not taken into account and interfering proteins (keratins) were eliminated. Quantitative data were normalized based on the abundance of precipitated EIF2A. Proteins with an abundance ratio >2 were considered over-abundant. The experiments were performed three times and the obtained results were compared. In addition, western blot was performed in a similar experimental method to confirm effectiveness and inter-sample comparability of EIF2A immunoprecipitation process.

2.11. Pulsed-stable isotope labeling by amino acids in cell culture (pSILAC)

As a version of the canonical SILAC approach, a pulse marking was carried out. L-Azidohomoalanine (AHA), a methionine analogue that allows rapid and sensitive enrichment of peptides by click-chemistry reaction, was used to isolate only newly synthesized proteins. CBCA-treated glioblastoma cells were used as negative control. The results obtained on these three systems were compared with those achieved on untreated wild-type glioblastoma cells. To perform p-SILAC experiments, the cells were washed twice with PBS and then incubated in depletion media (reduced component DMEM) for 30 min and then treated with Heavy (Lys8-Arg10) or Intermediate (Lys4-Arg6) medium in the presence of 0.1 mM AHA and the specific compounds (CBDA, CBCA or DMSO) at 50 μM for 4 h. Then, the cells were harvested in cold PBS and pelleted. The lysate was obtained by resuspending the cells in urea lysis buffer and sonicated with a probe sonicator. Finally, the cycloaddition enrichment was performed according to the instructions of the manufacturer. Proteins were eluted from the beads and subjected to trypsin digestion. The peptides were cleaned up using an Oasis PRiME HKB μElution Plate, dissolved in 0.1 % trifluoroacetic acid and analyzed by LC-MS/MS. The mass spectrometry analyses were performed as described in Limited proteolysis paragraph. MaxQuant analysis was performed setting number of maximum missed cleavage site to 2 and the minimum peptide length was reduced to 2. The SILAC ratios of proteins obtained from the MaxQuant searches were imported into Perseus software (version 1.5.2.3). To eliminate contamination and reverse identifications, these were filtered out, and the remaining protein SILAC ratios were transformed using a Log2 method. To perform statistical analysis, the SILAC ratios of each protein were analyzed separately to identify significant changes in protein expression between different experimental conditions. Quantification was performed using only those proteins that were present in at least 75 % of replicates in at least one condition, and missing values were imputed with random numbers from a normal distribution (1.8, 0.3). Welch's test in Perseus was used to identify significantly changed proteins between regions, with a significance threshold set at $p < 0.05$. Pearson correlations were calculated through the multiscatter plot function in Perseus. Hierarchical clustering was plotted using heatmap function in RStudio (version 2022.07.2) based on Euclidean distance to group the proteins based on their expression patterns. Enriched gene ontology (GO) terms and pathways were identified through ShinyGO 0.8 software [39] using Fisher's exact test with Benjamini-Hochberg FDR 0.1, with total quantified proteins serving as the background. These methods were employed to identify potential biological processes and pathways that may be altered between the experimental conditions.

2.12. Expression level of EIF2A, pEIF2α and GRP78

Cells were seeded $2*10^5$ per well in 6-well plates in 10 % FBS-DMEM. The next day, cells were treated with 50 μM CBDA or 0.1 % (*v*/v) DMSO in the presence of 0 %–1.5 %–10 % FBS for 4 h. The cells were lysed in RIPA buffer. The proteins were separated by a 12 % SDS-PAGE and western blot analysis was carried out. Nitrocellulose membranes were incubated with the specific antibodies. The protein bands were detected by enhanced chemiluminescence. Densitometric analyses of the resulting bands were carried out using the ImageJ software. GAPDH and actin were used as a normalizer.

2.13. Measurement of the levels of p62, LC3I/LC3II and ubiquitination

U87MG cells were seeded $1.8*10^5$ per well in 6-well plates while NHA were seeded $6.0*10^4$ per well in 12-well plates. The next day, cells were treated with 50 or 100 μM CBDA or 0.1 % (*v*/v) DMSO for 24 h. The cells were lysed as described above. For the measurement of the expression levels of p62 and LC3I/LC3II, the proteins were separated by a 15 % SDS-PAGE and western blot analysis was carried out. Instead, for the measurement of ubiquitination, the proteins were separated by an 8 % SDS-PAGE. Nitrocellulose membranes were incubated with the specific antibodies. The protein bands were detected by enhanced chemiluminescence. Densitometric analyses of the resulting bands were carried out using Chemidoc software (BioRad). GAPDH or Tubulin were used as normalizer.

3. Results

3.1. CBDA targets Eukaryotic Initiation Translation Factor 2A (EIF2A) in a glioblastoma cell line

To shed light on the biological effect of CBDA in tumor cells, we performed a chemical proteomics study, selecting U87MG with epithelial morphology as a representative glioblastoma cell line. Preliminarily, the cytotoxicity of CBDA against glioblastoma cells was evaluated. When we assayed the phytocannabinoid on U87MG cells grown under optimal conditions (DMEM supplemented with 10 % FBS), we observed negligible effects on cell viability at CBDA concentration up to 50 μM (Fig. S2A). The antiproliferative activity of phytocannabinoids against cancer cells is often tested in the presence of low amounts of FBS [40,41]. Therefore, we also carried out the MTT assay on U87MG cells in the presence of 1.5 % and 0 % FBS, to minimize the putative reduction in CBDA bioavailability due to serum components. However, under these conditions, we recorded a decrease in cell proliferation even in the presence of 0.1 % DMSO, and this effect was significantly enhanced by CBDA. (Fig. S2B). Based on these results, and since the studies aiming at defining the target of a bioactive compound should be performed under conditions that negligibly affect cell viability [40],we choose to carry out all subsequent experiments on U87MG cells cultivated in the presence of 10 % FBS, and using the higher amount of CBDA not producing signficant antiproliferative effects (50 μM).

To identify the putative protein targets of CBDA, we used Drug Affinity Responsive Target Stability (DARTS) experiments coupled with

LC/MS/MS analyses. DARTS is a proteomic-based assay exploiting the increased resistance to enzymatic proteolysis of a protein upon its interaction with a ligand [42]. The identification of proteins with decreased proteolytic susceptibility after CBDA treatment allowed us to identify the putative interactors of the phytocannabinoid. We performed this analysis on intact cells and several putative candidates emerged (Table S1). Gene ontology analysis showed that almost all of these proteins are involved in translation and related processes (Fig. 1B,C) while protein-protein interaction network-based investigation indicated that some of them interact directly between them in a more or less stable way (Fig. 1D). In particular, we considered the protein participating in the Eukaryotic Translation Machinery (ETM) [43–45] and the Eukaryotic Initiation Translation Factor 2A (EIF2A) as very promising putative targets. Previous studies have shown that phytocannabinoids can modulate ER stress [46] and the EIF2A-mediated activation of the ETM regulates the cellular response to different stress conditions [43]. Therefore, the ability of CBDA to modulate the activity of EIF2A and/or ETM proteins could actually underlie the biological effect of this compound. To confirm this hypothesis, preliminarily we verified the intracellular interaction between CBDA and these putative targets using DARTS assays coupled with western blot analyses, and selecting the Eukaryotic Elongation Factor 1 gamma (EEF1G) for its involvement in the ETM (Fig. 1E). The obtained results confirmed the ability of CBDA to protect both EIF2A and EEF1G from proteolysis.

We investigated further the putative interaction between CBDA and EIF2A and EEF1G by Cellular Thermal Shift Assay (CETSA) [47] in U87MG cells. We either incubated the cells with CBDA or let them untreated for 4 h, and subsequently we heated them for 5 min at different temperatures (53–60 °C). We then subjected the cells to non-denaturing lysis and measured the residual amount of soluble EIF2A and EEF1G by WB (Fig. 2A). The comparison between untreated and CBDA-treated samples showed that the phytocannabinoid was able to induce stabilization of both the proteins already at 56 °C, as inferred by the higher amounts of soluble EIF2A and EEF1G detected in the treated samples at that temperature (Fig. 2B and Fig. S3). This protective effect persisted at higher temperatures, becoming negligible only at 60 °C.

The DARTS and CETSA experiments allowed us to study the interactions between CBDA and proteins in their cellular environment and the results obtained reflected the accessibility of proteins by the phytocannabinoid. However, because the identified target proteins directly or indirectly interact with each other in cells, the results obtained did not allow us to define whether CBDA binds one or more proteins. In fact, the observed effects could be determined by a direct link between phytocannabinoid and proteins but also by the stabilization of the

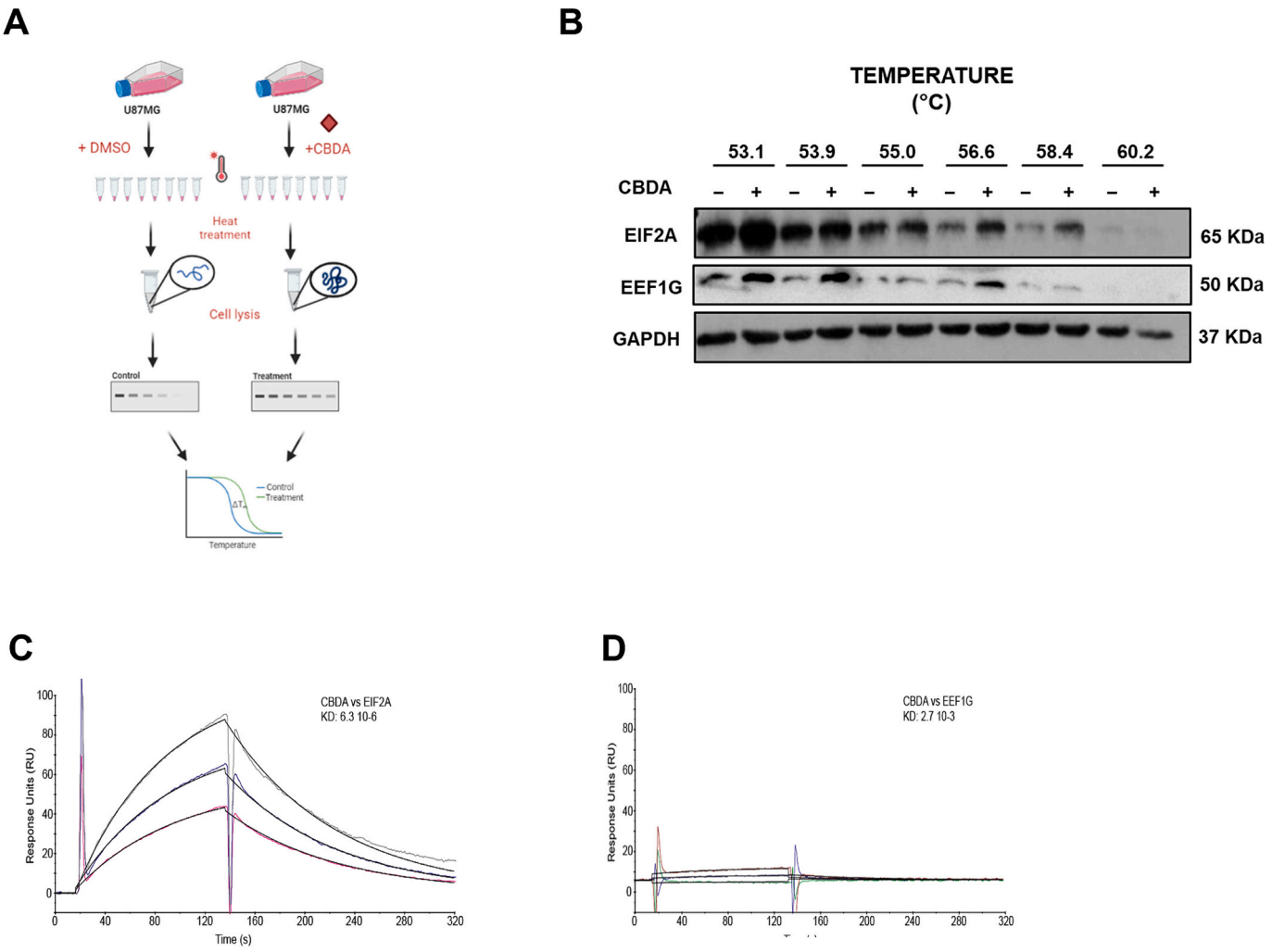

Fig. 2. Validation of CBDA/EIF2A interaction A) Cellular thermal Shift Assay (CETSA) workflow; B) Western blot analysis of soluble amount of EIF2A and EEF1G in CETSA performed on U87MG cells incubated with 50 μM CBDA or with the vehicle, in the range of temperature 53.1–60.2 °C; C) SPR sensorgrams obtained for the interaction of EIF2A with CBDA obtained by injecting three different concentrations (1 μM, 5 μM and 20 μM) of the cannabinoid on the immobilized protein; D) SPR sensorgrams obtained for the interaction of EEF1G with CBDA obtained by injecting three different concentrations (1 μM, 5 μM and 20 μM) of the cannabinoid on the immobilized protein.

binding between EIF2A and the ETM proteins. Thus, we performed Surface Plasmon Resonance (SPR) analyses to monitor the direct interaction between CBDA and EIF2A or EEF1G in real time. The results obtained confirmed that CBDA binds effectively to EIF2A, as deduced from the dissociation constant (K_D) of 6.3 μM measured for the EIF2A/CBDA complex (Fig. 2C). Conversely, the sensorgrams obtained by injecting CBDA onto immobilized EEF1G (Fig. 2D) demonstrated that the affinity of the cannabinoid for that protein was negligible. Although it cannot be excluded that it may depend on the experimental conditions, this result suggested that the EEF1G stabilization observed in the DARTS and CETSA experiments could be due to an indirect effect, possibly mediated by EIF2A.

Based on these data, we decided to investigate further the CBDA/EIF2A interaction and its biological consequences on the activity of the protein in the context of glioblastoma cells. As a first step, to evaluate if EIF2A ability to bind CBDA was specific, we performed again the DARTS, CETSA and SPR assays, according to the same experimental protocols described above, using cannabichromenic acid (CBCA) (Fig. 3A). Although both CBDA and CBCA are meroterpenoids characterized by the presence of a hydroxylated benzoic acid, CBCA carries a chromene ring. Consequently, the CBCA structure is significantly more planar than that of CBDA. All the obtained results (Fig. 3 B-D) clearly showed that CBCA has no ability to interact with EIF2A nor to stabilize the protein in the cell, thus indicating a certain selectivity in the recognition of the ligand by EIF2A, in which a critical role might be played by the planarity of the small molecule.

Finally, we tested whether the ability of CBDA to interact with EIF2A depended on the tumor nature of the cell line analyzed. Therefore, we performed the DARTS experiment on normal human astrocytes (NHA), a non-tumor cell line of the central nervous system, and no protection of EIF2A from protease action due to phytocannabinoid treatment was detected (Fig. S4).

3.2. CBDA binding induces significant conformational changes in EIF2A, anchoring the flexible α-helix 482–502 to the WD domain

Limited proteolysis followed by mass spectrometry (LiP-MS) provides information on protein conformational changes following intermolecular binding, on a proteome-wide scale and in a complex biological and pseudo-physiological environment [48]. To identify the region of interaction between CBDA and EIF2A, we performed LiP-MS on the CBDA-EIF2A complex. In particular, we incubated the U87MG cells with CBDA for 4 h or let them untreated (as a control), and then performed a subtilisin-catalyzed digestion under optimized conditions followed by a complete tryptic digestion (Fig. 4A). In this approach, the EIF2A region interacting with CBDA was protected from subtilisin-catalyzed digestion and thus hydrolyzed exclusively by trypsin. Conversely, unprotected regions were susceptible to both proteolysis steps. Therefore, tryptic fragments of the EIF2A region involved in CBDA binding were expected to be detected only in the treated sample and not in the control. In fact, more tryptic fragments were identified in samples treated with CBDA than in control, thus suggesting that this compound could induce an overall protein resistance to proteolysis (Table S2). Specifically, the EIF2A region primarily affected by CBDA binding was the C-terminus, as inferred by the three tryptic peptides (425–441, 461–482 and 521–536) detected exclusively in the treated sample (Fig. 4B).

We then used these data to guide the structural modeling of the EIF2A-CBDA complex. We obtained a three-dimensional (3D) model of the full-length protein (1–585 aa) from AlphaFold database. Based on the prediction, EIF2A protein consists of a N-terminal WD-repeat domain organized in a circularly-arranged nine-bladed β-propeller

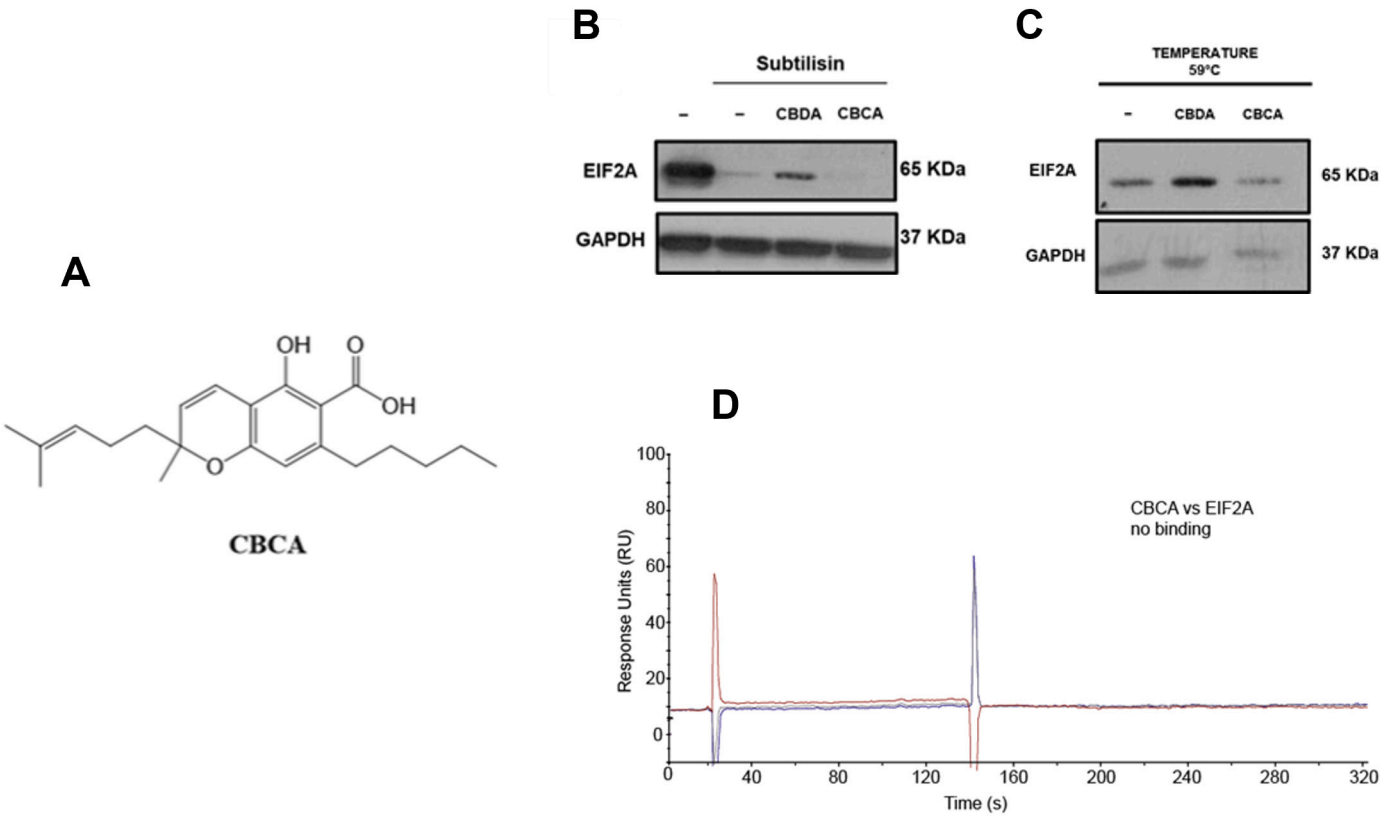

Fig. 3. Study of the binding between EIF2A and CBCA A) Chemical structure of cannabichromenic acid (CBCA) B) Western blot analysis of DARTS experiment carried out on U87MG treated with 50 μM CBDA or CBCA, using anti-EIF2A antibody. GAPDH was used as a control; C) Western blot of soluble amount of EIF2A in CETSA experiment performed on U87MG cells treated with 50 μM CBDA or CBCA and then incubated at the temperature of 59 °C; D) SPR sensorgrams obtained for the interaction of EIF2A with CBCA obtained by injecting three different concentrations (1 μM, 5 μM and 20 μM) of the cannabinoid on the immobilized protein.

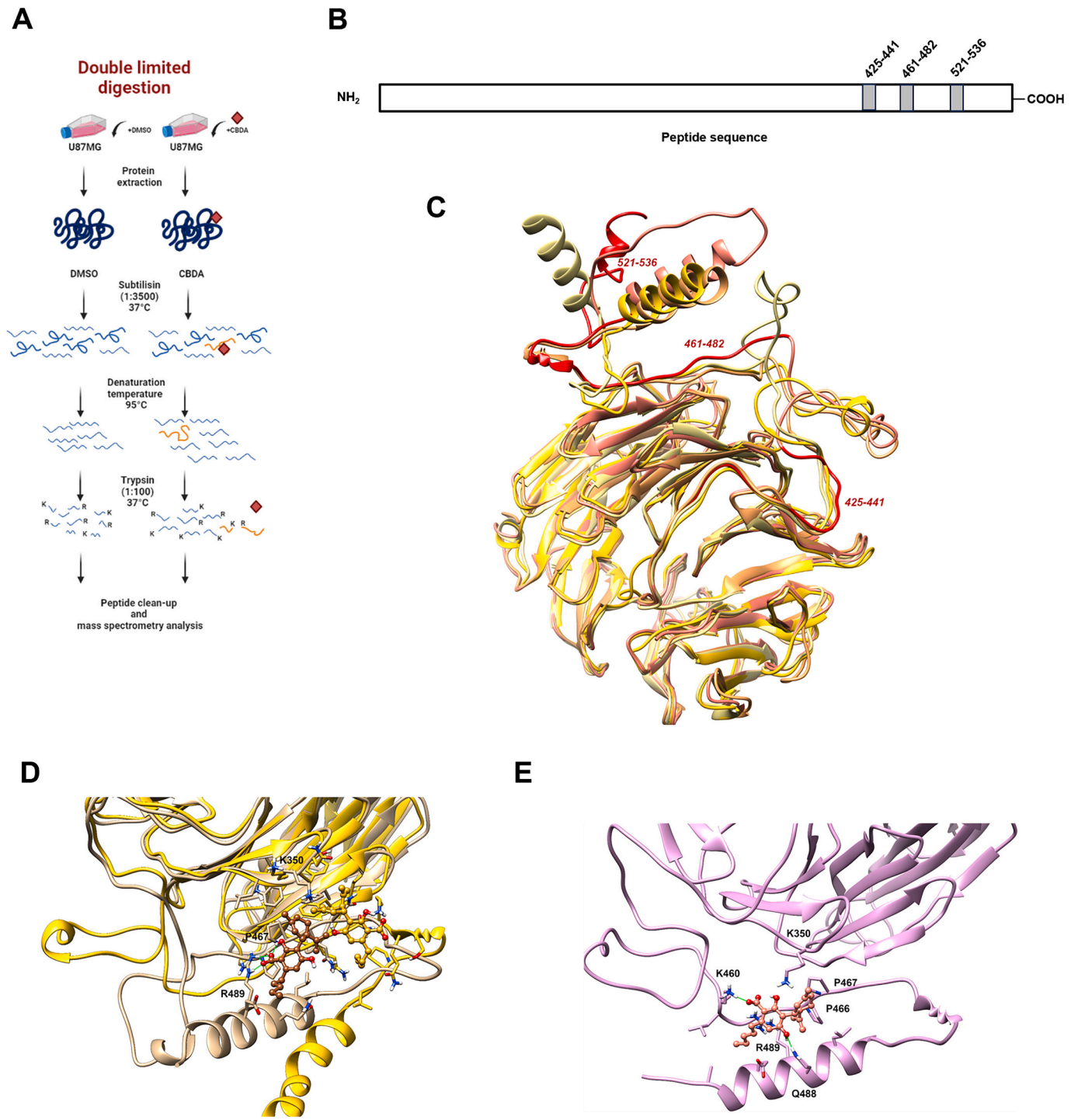

Fig. 4. EIF2A region involved in CBDA binding A) Mass-spectrometry Limited proteolysis (MS-LiP) experimental workflow for double-limited digestion; B) Protein regions emerged from limited proteolysis experiments as protected (in gray) following EIF2A interaction with CBDA. The intensity of the respective peptides are reported in the graph; C) Best fit at the level of WD-domain of MD frames taken every 100 ns over the full-simulated period (400 ns). The three tryptic peptides (425–441, 461–482 and 521–536) are colored in red and shown only for the 400 ns MD frame for clarity. The C-terminal coiled coil next to site 3 has been omitted for clarity; D) Best fit at the level of backbone atoms of WD domain between the starting docking complex (yellow) and the representative MD frame (tan). CBDA is painted gold in the docking complex and brown in MD complex. H-bonds are shown as green lines. Residues within 4 Å from the ligand are shown in stick. Hydrogen, oxygen and nitrogen atoms are painted white, red and blue, respectively. The C-terminal coiled-coil has been omitted for clarity; E) Representative frame from UnrDisRes-site2 MD of CBDA-EIF2A complex. Residues within 4 Å from the ligand are shown in stick. Hydrogen, oxygen and nitrogen atoms are painted white, red and blue, respectively. H-bonds are shown as green lines. The C-terminal coiled-coil has been omitted for clarity.

fold, formed by four-stranded antiparallel β-sheet motifs (1–415), followed by a poorly structured region which includes an α-helix and a C-terminal coiled-coil (530–580). During this study, the x-ray structure of the human WD-repeat domain was released (PDB id: 8DYS). The Molecular Dynamics (MD) trajectory analysis showed that a stretch of residues (463–472 aa) within the site2 region forms a stable additional strand of the WD domain and aligns in an antiparallel manner to the 307–315 β-strand (Fig. 4C). Indeed, some residues belonging to the

463–472 stretch engage stable H-bonds, diagnostic of a β-strand with the flanking region 307–317: the backbone carbonyl and amide groups of Gln468 with the correspondent backbone groups of Asp311 (occurrence >74 %), the amide group of Glu465 with Thr314 carbonyl group (occurrence ~20 %), the amide group of Met470 with the carbonyl group of Val309 (occurrence >40 %), while the sidechains of Glu464 and Glu464 engage H-bonds with Thr314 sidechain and/or backbone. Moreover, α-helix 482–502 progressively reorients towards the 463–472 stretch during MD, potentially contributing to the CBDA binding site. Loop 425–441 (site1) stably packs against the β-sheet domain, stabilized by a network of H-bonds involving the following pairs of residues: Thr427-Tyr392 (backbone-sidechain, >25 %), Tyr428-Asp345 (sidechain-sidechain, >85 %), Val431-Ser395 (backbone-sidechain, >94 %), Glu435-Ile396 (backbone-backbone, >47 %), Pro436-Lys399 (backbone-sidechain, >30 %), Asn337-Gly394 (sidechain-backbone, >14 %), Lys441-Lys354 (backbone-backbone >48 %). Site3, encompassing residues 521–536, albeit including a stretch of residues in α-helix (531–535) represents the most flexible region among those identified by LiP-MS, being unanchored to the N-terminal domain.

To find the putative binding mode of CBDA to the EIF2A protein, a representative frame from the last 100 ns of free protein MD trajectory was selected as target for docking studies, focused on each stretch of residues previously identified by LiP-MS as a putative binding site (sites1–3). The three docking complexes, obtained selecting the CBDA best poses in terms of binding energy, underwent up to 200 ns of unrestrained MD simulations to assess the stability of the binding pose, also allowing possible rearrangements of the ligand (MD trajectories UnrDock-site1, UnrDock-site2 and UnrDock-site3). To assess further the binding region for CBDA, a complementary MD-based approach was pursued, using as starting coordinates the dissociated complex, with the compound placed 40 Å apart from the binding site. For each target region, time-dependent distance restraints between the ligand carbon atom bound to the terpenoid ring and the Cα atoms of each selected region were applied during the first 100 ns of MD, followed by 100 ns of unrestrained MD, to maximize the exploration of the conformational space around the three regions of interest (MD trajectories UnrDisRes-site1, UnrDisRes-site2, UnrDisRes-site3). The analysis of UnrDock-site1–3 MD trajectories showed that a stable binding is only obtained for site2. After an initial rearrangement, CBDA fits stably in this site during the remaining simulated time in UnrDock-site2 trajectory (Fig. S5A), grafting together the stretch of residues 463–472, flanking the β-strand 307–315 of the WD domain, and the adjacent 482–502 α-helix, which thus gets closer to the strand. In this new pose, CBDA binding is stabilized by its ionic interaction with Arg489, lying on the α-helix, and by hydrophobic stacking interactions of CBDA aromatic and terpenoid rings with Pro466 and Pro467, respectively (Fig. 4D). The CBDA pentyl chain also contributes to the pattern of hydrophobic interactions with Leu485 and Arg489 side chains. This result agrees with the lower affinity towards EIF2A observed in DARTS experiments for CBDVA, which carries a propyl instead of a pentyl moiety. To evaluate the reduction of the α-helix overall mobility induced by CBDA binding, the rmsd of this region was evaluated after best fit of the stretch residues 463–472 over the last 100 ns of UnrDock-site2 MD and compared with the values calculated over the last 100 ns of the MD simulation of the protein alone. As shown in Fig. S5B, the fluctuations of the α-helix at level of backbone atoms are strongly dampened when in complex with CBDA. Moreover, the solvent accessible surface of the stretch 463–472 is also reduced upon binding (383 ± 0.18 Å2 vs 703 ± 0.33 Å2 over the same time interval above mentioned. The analysis of UnrDisRes-site1–3 MD trajectories showed binding modes at site2 substantially overlapping those from MD after docking, confirming the region between the proline residue 466–467 and the nearby α-helix as the putative binding site for CBDA (Fig. 4E and Fig. S5C). In this pose, CBDA engages a π-cationic interaction with Arg489, an H-bond with Lys460 sidechain involving its carboxylate group and an H-bond with Gln488. The ligand in UnrDisRes-site1 and UnrDisRes-site3 trajectories moves in a region located approximately in the middle of the two original sites, closer to site2 (Fig. S5D-S5F).

In view of these results, the net effect of CBDA on the protein function could be explained by the ability of CBDA to stabilize the packing of the flexible α-helix 482–502 against the WD domain, ability due to the peculiar, tilted structure of CBDA, and thus not observed for the more planar CBCA.

3.3. CBDA-induced conformational rearrangement modifies EIF2A interactome

Given the significant changes occurring in the EIF2A structure upon the cannabinoid binding, treatment of glioblastoma cells with CBDA was expected to impact on EIF2A affinity for its interaction partners. Therefore, we carried out a co-immunoprecipitation (Co-IP) protocol on cell lysates from U87MG cells treated with either CBDA or vehicle alone. Preliminarily, we verified that the treatment did not affect the intracellular level of EIF2A (Fig. 5A) and that the efficiency of the immunoprecipitation procedure on this protein was the same in the different samples (Fig. 5B).

Mass spectrometry-based analysis of the resulting mixtures led to the identification of 28 proteins (Table 1). Among them, we detected several previously described/supposed EIF2A interactors (i.e. Elongation factor 1-alpha, Elongation factor 2, ATP dependent RNA helicase, 40S ribosomal proteins, GRP78) [49,50]. However, our analysis also shed light on partners never described before, including molecular chaperones (T complex proteins, Hsp60, Hsp71, Hsp90 and 14-3-3) and proteins participating in granules and vesicles formation and trafficking (annexins, RABs, T complex proteins).

To evaluate whether the binding to CBDA perturbates EIF2A interactome, we performed a quantitative mass spectrometry analysis and we compared the protein abundance in EIF2A co-immunoprecipitates from CBDA-treated and control cells. Notably, the abundance of some of the partner proteins increased upon CBDA treatment (Table 1) thereby indicating that CBDA binding induced a stabilization of specific protein-protein interactions involving EIF2A. In particular, we measured higher amounts of proteins belonging to the eukaryotic translation machinery (i.e. EEF1G, EEF1D, EEF1A1, RPS2 and RPS6) (Fig. 5C), thus suggesting that CBDA treatment induces a stabilization of the binding between EIF2A and the protein complexes involved in translation initiation and protein chain elongation. As the interaction between EIF2A and ETM proteins was reported to be induced by EIF2α inactivation upon generic cell stress conditions [43], we monitored the changes in two markers of stress that might be induced by treatment with CBDA: the phosphorylation levels of EIF2α and abundance of GRP78. Comfortingly, up to 24 h incubation of U87MG cells with the cannabinoid did not significantly affect the p-EIF2α/EIF2α ratio and GRP78 concentration (Fig. 5D-E), thus confirming that CBDA was not a stress inducer. This result confirmed the increased resistance to proteolysis that we observed for several ETM components in the DARTS assay and the enhanced thermal stability of EEF1G emerged in CETSA might represent secondary effects of the CBDA-EIF2A binding.

3.4. Activation of EIF2A by CBDA modifies the nascent proteome of glioblastoma cells

The EIF2A activation has been reported to be responsible for important changes at the translational level [51]. Therefore, the results we obtained prompted us to investigate the repercussions of the glioblastoma cells treatment with CBDA on the translation-initiation-factor activity of EIF2A. To this end, we conducted pulsed SILAC experiments based on AHA-click chemistry [52] to specifically evaluate the impact of CBDA treatment on the translation process in glioblastoma cells (Fig. 6A). This approach allows to carry out a differential proteomic analysis exclusively concerning the newly synthesized proteins in a given time interval, thus enabling to evaluate the result of a treatment

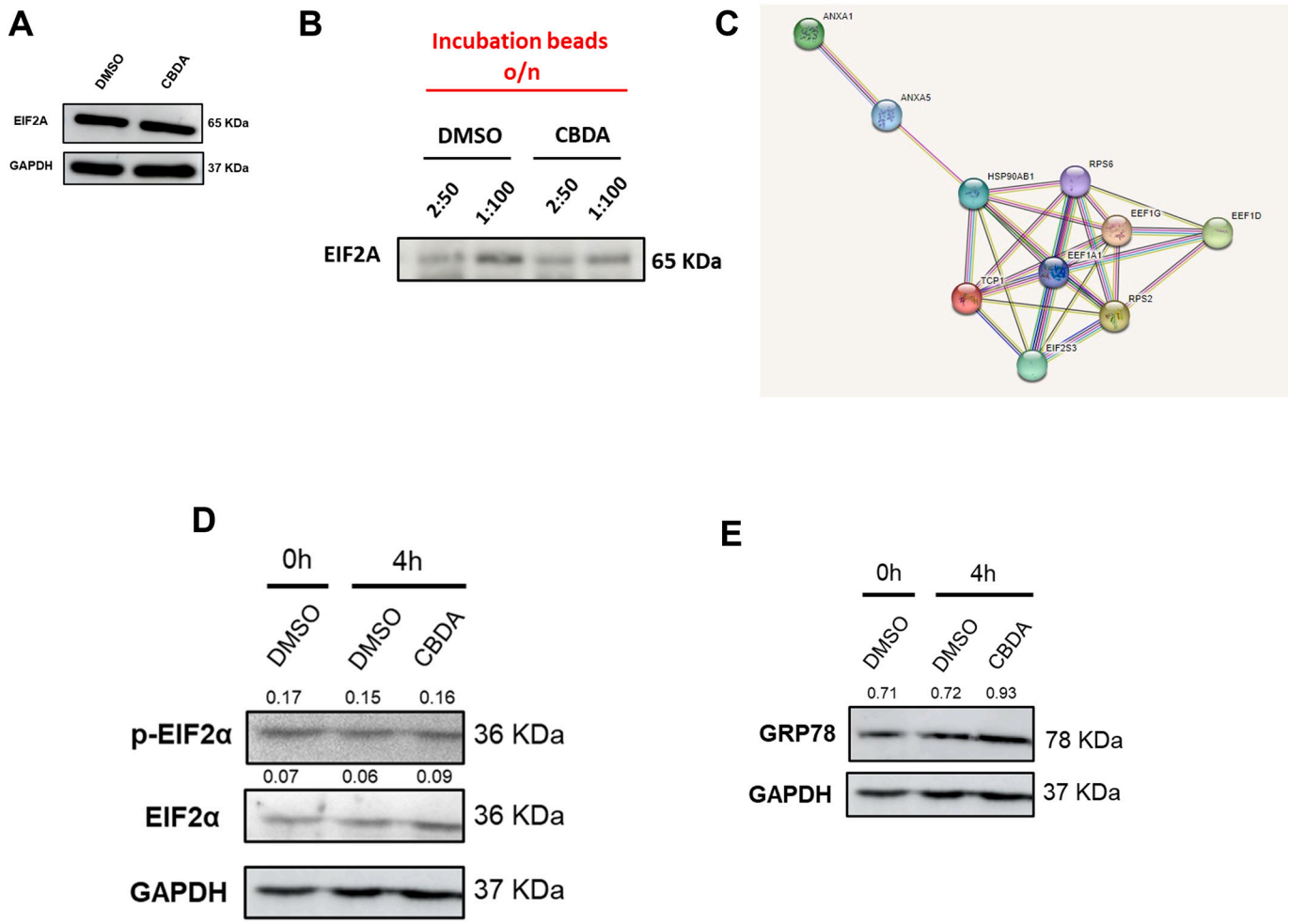

Fig. 5. EIF2A interactome is affected by CBDA binding A) EIF2A expression level of CBDA-treated U87MG cells after 4 h of incubation; B) WB analysis of EIF2A obtained by the immunoprecipitation procedure carried out on protein lysates obtained from U87MG cell underwent incubation with different amounts of CBDA or with the vehicle; C) Functional network analysis of the proteins whose affinity towards EIF2A was enhanced by CBDA treatment; D) p-EIF2α and EIF2α expression level in U87MG cells subjected to a 4 h incubation with CBDA or with the vehicle; E) GRP78 expression level in U87MG cells subjected to a 4 h incubation with CBDA or with the vehicle.

on the nascent proteome of a given biological system. To focus only on the effects directly dependent on CBDA interaction with EIF2A and to reduce the interference ascribable to secondary cellular responses, we chose a pulse time of 4 h. In parallel, we adopted glioblastoma cells treated with CBCA as a negative control. For each of the tested conditions, the effects of the treatment were evaluated in terms of changes in newly synthetized proteins compared to untreated U87MG cells.

We identified about 2500 newly synthesized proteins (Table S3), most of which were detected in all the samples. However, a quantitative analysis of the data revealed a clearly different effect of the glioblastoma cells incubation with the two phytocannabinoids (Fig. 6B), confirming again that CBDA and CBCA act on distinct target protein(s). In more detail, we identified nearly 100 proteins significantly modulated in CBDA treated samples (Table S4), while CBCA treatment affected the expression level of 151 proteins and only 9 proteins were modulated similarly by both the treatments. As expected from the previously described role played by EIF2A, the expression level of several molecular chaperones involved in unfolded protein response (UPR) (NPLOC4, DNAJC7, HSPA4L, PFDN5) was significantly enhanced upon glioblastoma cells incubation with CBDA. Furthermore, also the expression of proteins involved in intracellular vesicle formation and trafficking (e.g. DYNC1I1, DYNC1I2, ERC1, EXOC7, PRRC2C, RAB23, RIN1, RRAS, SNX1, TOM1L2, TSG101, VAPA) [53–59] was modified. A gene ontology-based analysis of the pSILAC results allowed us to define the cellular functions of proteins whose expression was affected by CBDA treatment (Fig. 6C and D). Two main clusters emerged from this analysis: proteins involved in nucleic acid translation and transcription, and proteins acting on protein catabolism in which ubiquitination plays a pivotal role. This latter appeared to be the most affected biological process, as demonstrated by the finding that 17 (i.e. AURKB, CNOT4, CPSF7, DDX1, FBL, H3—3B, NIFK, NOL7, RPS14, RPS3A, SH3KBP1, SMARCA1, SNW1, SP100, SRSF6, TSG101, UBE2S) out of the 67 up-regulated proteins are at different levels involved in the protein ubiquitination process. Based on these data, we evaluate the effect of a 24-h incubation of U87MG cells with CBDA on protein ubiquitination. The resulting WB (Fig. 6E) demonstrated the global amount of ubiquitinated proteins was increased following the treatment. To evaluate whether CBDA was able to induce a similar this effect also in non-tumor cells, we carried out the same analysis using NHAs. Remarkably, the level of ubiquitinated proteins in these cells following a 24-h exposure of to CBDA or 0.1 % DMSO was almost comparable (Fig.S6). This result and the output of DARTS performed on the same cells (Fig. S4) suggested that CBDA-mediated activation of EIF2A occurs mainly in cancer cells. Since the activation of protein ubiquitination [60], as well as the intracellular vesiculation [61], are linked to autophagy, we evaluated a possible impact of U87MG cells exposure to CBDA on that process. Therefore, we monitored the intracellular level of well-characterized autophagy markers: the isoforms I and II of Microtubule-associated

Table 1
Proteins identified in the co-immunoprecipitation experiments. The observed fold change was also reported: data were normalized on EIF2A abundance. The proteins that were more abundant after CBDA treatment were highlighted in yellow, those that were less abundant in light blue ($p < 0.05$).

Description	Fold change following CBDA treatment	*p value*
T-complex protein 1 subunit alpha (TCP1)	12.0	0.002
Elongation factor 1-gamma (EEF1G)	7.7	0.012
40S ribosomal protein S6 (RPS6)	4.1	0.013
Elongation factor 1-delta (EEF1D)	3.5	0.025
Annexin A5 (ANXA5)	3.2	0.018
40S ribosomal protein SA (RPS2)	3.2	0.015
Annexin A1 (ANXA1)	2.9	0.028
Heat shock protein 90kDa alpha (HSP90AB1)	2.7	0.025
Elongation factor 1-alpha (EEF1A1)	2.7	0.031
Member RAS onocogene family, isoform CRA_c (RAB15)	1.4	0.228
14-3-3 protein beta/alpha (YWHAB)	1.4	0.232
GTP-binding nuclear protein Ran (RAN)	1.4	0.353
Member RAS oncogene family, isoform CRA_a (RAB11A)	1.4	0.326
L-lactate dehydrogenase (LDHA)	1.3	0.519
78 kDa glucose-regulated protein (GRP78)	1.3	0.707
Alpha-enolase (ENO1)	1.3	0.692
Elongation factor 2 (EEF2)	1.1	0.855
Annexin A2 (ANXA2)	1.1	0.816
Heat shock cognate 71 kDa protein (HSPA8)	1.0	0.944
Eukaryotic translation initiation factor 2A (EIF2A)	**1.0**	**0.939**
Pyruvate kinase (PKM)	1.0	0.971
Caspase 14, apoptosis-related cysteine peptidase (CASP14)	1.0	0.892
Glyceraldehyde-3-phosphate dehydrogenase (GAPDH)	0.9	0.884
Arginase-1 (ARG1)	0.9	0.903
Protein-L-isoaspartate(D-aspartate) O-methyltransferase (PCMT1)	0.7	0.213
Triosephosphate isomerase (TPI)	0.7	0.326
60 kDa chaperonin (HSP60)	0.5	0.109
Heat shock protein beta-1 (HSPB1)	0.5	0.278
ATP dependent RNA helicase (DHX9)	0.2	0.043

protein 1A/1B-light chain 3 (LC3-I and LC3-II) and Sequestosome-1 (p62). Following a 24-h incubation of U87MG cells with CBDA, a significant increase of the amount of p62 and slight increment in the total quantity of LC3 was observed (Fig. 6F). Besides, the conversion of LC3-I to LC3-II was augmented by the treatment. This result suggested that CBDA induces the autophagosome formation in glioblastoma cells, but not its subsequent degradation [62,63].

4. Discussion

The identification of the molecular target(s) of a bioactive compound can provide information at three different levels: it obviously opens the way to the definition of the mechanism of action of the compound, leads to the discovery of new potential protein preys for therapeutic procedures and allows studying the functions of the target protein in its cellular environment. To obtain most of this information, proteomics-based methods represent the gold standard, since they are intrinsically unbiased and make it possible to study the interactions of a bioactive agent under pseudo-physiological conditions and even within cells while minimizing the risk of artifacts [30].

Here, we combined proteomic, biochemical, biophysical, computational and bioinformatic methods to investigate the bioactivity of CBDA in a glioblastoma human cell line, with the primary aim to identify the molecular target(s) of the phytocannabinoid. In order to detect only interactions that could actually occur within the cellular context, the experiments were carried out on intact and viable cells. Moreover, although studies of phytocannabinoid activity are often conducted under conditions that maximize the cytotoxic activity of these compounds [40,41], we performed all experiments using culture conditions that ensured optimal cell viability in an attempt to mimic the best pseudo-physiological conditions. Finally, we set up an experimental model allowing us to selectively identify CBDA specific protein interactors and to investigate direct and short-time related effects of the interaction with this phytocannabinoid. Therefore, we chose to perform the proteomic-based experiments using a relatively short incubation time of the cells with CBDA (4 h), in order to discriminate the biological effects triggered directly by the binding of the CBDA with its target, from those due to the subsequent activation of cellular response pathways. Data from complementary experiments have demonstrated that CBDA directly interacts with EIF2A. In eukaryotic cells, early steps of the translation initiation process are regulated by EIF2 complex; it is composed by α subunit, that mainly regulated the translational process through phosphorylation at Ser 51, and β and ϒ subunits responsible for binding the other components of the ETM complex [43]. Upon different stresses (e.g. deprivation of amino acids, viral infection, ER stress), EIF2α undergoes phosphorylation at Ser51, thereby resulting in global

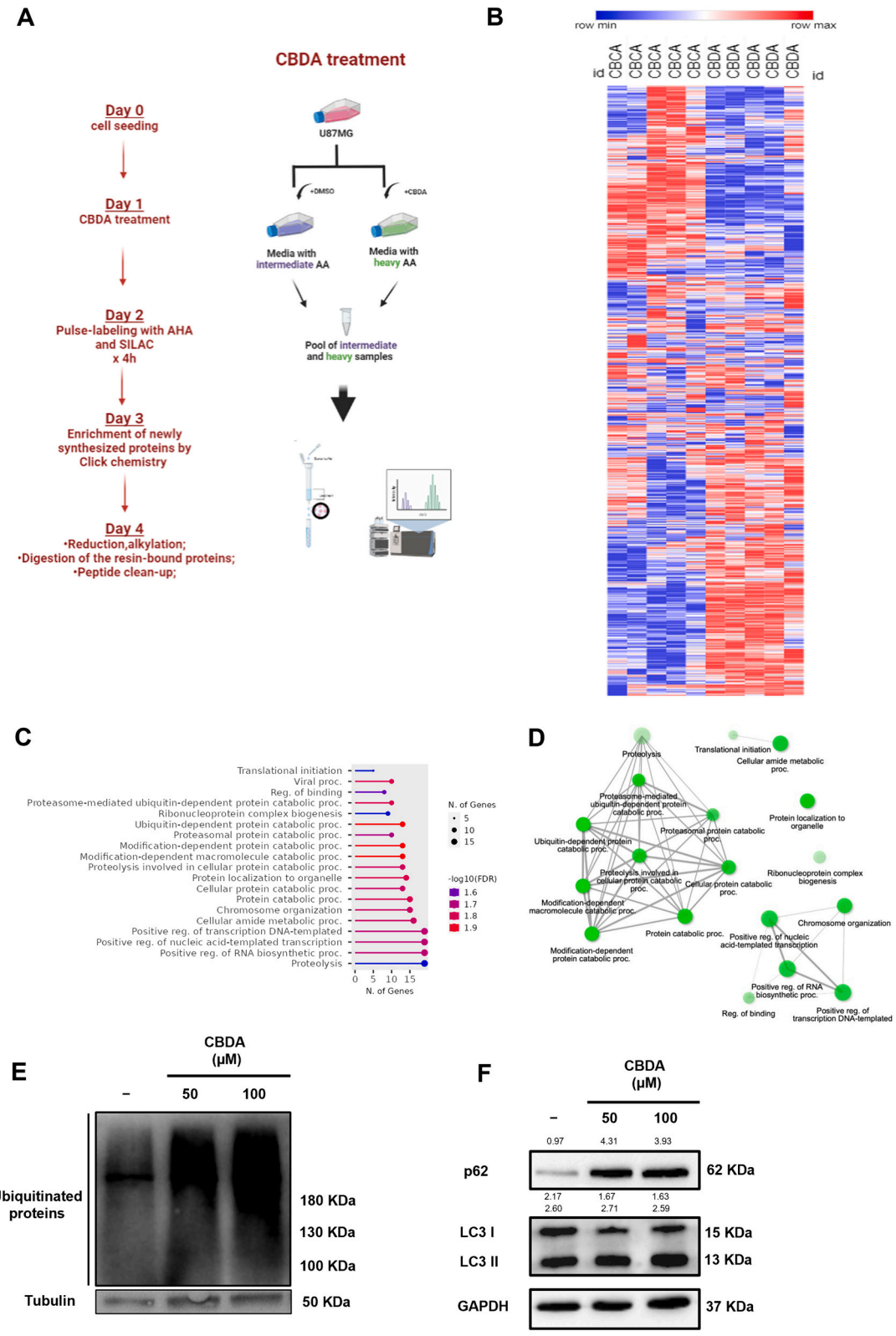

Fig. 6. Effect of CBDA treatment on the nascent proteome of U87MG cells A) Pulsed- Stable Isotope Labelling by Amino acids in cell culture (p-SILAC) workflow; B) heat-map representation of the results obtained by the p-SILAC experiments performed on U87MG cells treated with 50 μM CBDA or 50 μM CBCA; C) Biological functions of the proteins whose neosynthesis level was significantly modulated by U87MG incubation with 50 μM CBDA, clusterized by ShinyGO 0.8 software; D) Network of the biological functions of the proteins whose neosynthesis level was significantly modulated by CBDA; E) Western blot analysis of ubiquitinated proteins in cell subjected to a 24 h incubation with 50 μM or 100 μM CBDA or with the vehicle; F) Western blot analysis of p62 and LC3I and LC3II in cells subjected to a 24 h incubation with 50 μM or 100 μM CBDA or with the vehicle.

inhibition of protein expression and activation of the alternative initiation factor EIF2A [49]. EIF2A is required to translate the upstream open reading frames (uORFs) present in mRNAs controlled by the ISR, many of which have a non-AUG starting codon [64,65]. However, EIF2A was also reported to regulate the translation of selected cancer associated mRNA, thus having an important role in tumor progression [66]. As an example, Kwon and colleagues [67] showed that EIF2A is responsible for the translation of the mRNA of c-Src, a non-receptor protein tyrosine kinase, whose overexpression strongly correlates with the formation of solid tumors.

The results we obtained in this study indicated that the binding of CBDA to EIF2A generates a series of correlated events. First, it led to a rearrangement of the C-terminal region of the protein, reported to be important for the interaction with the 40S complex [68], thus increasing the affinity of EIF2A for the ETM proteins. Consequently, the nascent proteome of the glioblastoma cells was affected, and we observed the over-expression of several proteins involved in the cellular stress response, although no such stress occurred under the experimental conditions used. Based on our evidence it is therefore possible to hypothesize that CBDA acts as an activator of EIF2A, while under physiological conditions EIF2A activation is associated with EIF2α inhibition.

Remarkably, our study has provided new insights into the functions of EIF2A. In fact, our results of the co-immunoprecipitation and translational analysis via pulsed-SILAC confirmed the previously described interaction with the ETM proteins and the regulation of the expression of proteins involved in responses to cellular stress. Moreover, it also emerged that EIF2A has a pivotal role in the regulation of the protein homeostasis, by enhancing ubiquitination processes thus inducing a significant accumulation of the autophagosome. A correlation between EIF2A activation and autophagy has been previously reported in models different from ours [69,70], but the mechanism by which the protein modulated the process has never been discussed. Anderson et al. showed that in EIF2A-knockout mice the levels of p62 and LC3-II were reduced compared to wild type animals [70]. A comparison between our data and those obtained by Anderson and colleagues supports the hypothesis that the effects we observed following the CBDA treatment of the glioblastoma cells were mediated by an activation of EIF2A.

Altogether, the outputs of our research indicated that EIF2A can trigger various stress-related mechanisms, and that CBDA is able to push it by directly interacting with the protein. The resulting effects can have a very different biological outcome depending on the type of cells and the context in which they occur. On the one hand, in fact, it has been shown that modulation of p62 can play an important role in neuroprotection, and therefore EIF2A activation may have a preventive effect on some pathologies affecting the cells of the nervous system [71]. However, the imbalance of RNA and protein homeostasis, as well as the accumulation of the autophagosome, generated by the anomalous activation of EIF2A, could be critical for cells with an accelerated metabolism such as tumor ones. This may underlie the particular sensitivity of glioblastoma cells treated with CBDA to nutrient deprivation that we observed in experiments conducted in the presence of reduced amounts of FBS (Fig. S2B). Preliminary data we have obtained on U87MG cells incubated with very low (1.5 %) or no FBS are in agreement with this hypothesis. Indeed, even 4 h of incubation under these conditions induced cellular stress, as inferred by an increment of pEF2α and GRP78 levels (Fig. S7).

Abbreviations

CBCA	Cannabichromenic acid
CBD	Cannabidiol
CBDA	Cannabidiolic acid
CETSA	Cellular Thermal Shift Assay
Co-IP	Co-immunoprecipitation
DARTS	Drug Affinity Target Stability Assay
EEF1G	Eukaryotic Elongation Factor 1 gamma
EIF2A	Eukaryotic Initiation Translation Factor 2A
EIF2α	Eukaryotic Initiation Translation Factor 2 alpha
ETM	Eukaryotic Translation Machinery
FBS	Fetal bovine serum
GAPDH	Glyceraldehyde 3-phosphate dehydrogenase
GRP78	78 kDa glucose-regulated protein
LC3	Microtubule-associated protein 1A/1B-light chain 3
LiP	Limited proteolysis
MD	Molecular Dynamics
p62	Sequestosome-1
pSILAC	Pulsed-Stable Isotope Labelling by amino acids in cell culture
SPR	Surface Plasmon Resonance
U87MG	Human glioma cells (ECACC No: 89081402)
Δ9-THC	Δ9-tetrahydrocannabinol

Supplementary data to this article can be found online at https://doi.org/10.1016/j.ijbiomac.2024.132968.

CRediT authorship contribution statement

Maria Laura Bellone: Writing – original draft, Methodology, Formal analysis, Data curation, Conceptualization. **Azmal Ali Syed:** Formal analysis, Data curation. **Rosa Maria Vitale:** Writing – original draft, Software, Formal analysis. **Gianluca Sigismondo:** Formal analysis, Data curation. **Francesca Mensitieri:** Writing – review & editing. **Federica Pollastro:** Writing – review & editing, Resources. **Pietro Amodeo:** Software, Data curation. **Giovanni Appendino:** Writing – review & editing, Resources. **Nunziatina De Tommasi:** Writing – review & editing, Funding acquisition, Data curation. **Jeroen Krijgsveld:** Writing – original draft, Data curation. **Fabrizio Dal Piaz:** Writing – original draft, Supervision, Project administration, Data curation, Conceptualization.

Declaration of competing interest

The authors declare the following financial interests/personal relationships which may be considered as potential competing interests:

Nunziatina De Tommasi reports financial support was provided by Italian Ministry of Research and University. If there are other authors, they declare that they have no known competing financial interests or personal relationships that could have appeared to influence the work reported in this paper.

Data availability

The mass spectrometry proteomics data have been deposited to the ProteomeXchange Consortium via the PRIDE partner repository. Specifically, the dataset identifier of DARTS data is PXD043893, that of Co-IP data is PXD043947, for LiP data PXD043933 and that of pulsed-SILAC data is PXD043928.

Acknowledgments

This work was supported by MIUR, research grant PRIN2017, Project WN73PL (Bioactivity-directed exploration of the phytocannabinoid chemical space).

References

[1] E. Gianazza, I. Miller, U. Guerrini, L. Palazzolo, T. Laurenzi, C. Parravicini, I. Eberini, What if? Mouse proteomics after gene inactivation, J. Proteomics 199 (2019) 102–122, https://doi.org/10.1016/J.JPROT.2019.03.008.

[2] S. Ye, J. Wu, Y. Wang, Y. Hu, T. Yin, J. He, Quantitative proteomics analysis of glioblastoma cell lines after lncRNA HULC silencing, Sci. Rep. 11 (2021), https://doi.org/10.1038/S41598-021-92089-Z.

[3] S. Heinzlmeir, S. Müller, Selectivity aspects of activity-based (chemical) probes, Drug Discov. Today 27 (2022) 519–528, https://doi.org/10.1016/J.DRUDIS.2021.10.021.

[4] B.R. Stockwell, X. Jiang, The chemistry and biology of ferroptosis, Cell Chem. Biol. 27 (2020) 365–375, https://doi.org/10.1016/J.CHEMBIOL.2020.03.013.
[5] A. Saha, D. Bello, A. Fernández-Tejada, Advances in chemical probing of protein O-GlcNAc glycosylation: structural role and molecular mechanisms, Chem. Soc. Rev. 50 (2021) 10451–10485, https://doi.org/10.1039/D0CS01275K.
[6] R.S. Magin, X. Liu, A. Felix, A.S. Bratt, W.C. Chan, S.J. Buhrlage, Small molecules as tools for functional assessment of deubiquitinating enzyme function, Cell Chem. Biol. 28 (2021) 1090–1100, https://doi.org/10.1016/J.CHEMBIOL.2021.04.021.
[7] L.O. Hanuš, S.M. Meyer, E. Muñoz, O. Taglialatela-Scafati, G. Appendino, Phytocannabinoids: a unified critical inventory, Nat. Prod. Rep. 33 (2016) 1357–1392, https://doi.org/10.1039/C6NP00074F.
[8] L.A. Parker, E.M. Rock, C.L. Limebeer, Regulation of Nausea and Vomiting by Cannabinoids, 2011, https://doi.org/10.1111/bph.2011.163.issue-7.
[9] A.S. Kleckner, I.R. Kleckner, C.S. Kamen, M.A. Tejani, M.C. Janelsins, G.R. Morrow, L.J. Peppone, Opportunities for cannabis in supportive care in cancer, Ther. Adv. Med. Oncol. 11 (2019), https://doi.org/10.1177/1758835919866362.
[10] S. Zou, U. Kumar, Cannabinoid receptors and the endocannabinoid system: signaling and function in the central nervous system, Int. J. Mol. Sci. 19 (2018), https://doi.org/10.3390/IJMS19030833.
[11] M. Tham, O. Yilmaz, M. Alaverdashvili, M.E.M. Kelly, E.M. Denovan-Wright, R. B. Laprairie, Allosteric and orthosteric pharmacology of cannabidiol and cannabidiol-dimethylheptyl at the type 1 and type 2 cannabinoid receptors, Br. J. Pharmacol. 176 (2019) 1455–1469, https://doi.org/10.1111/BPH.14440.
[12] N. Mangal, S. Erridge, N. Habib, A. Sadanandam, V. Reebye, M.H. Sodergren, Cannabinoids in the landscape of cancer, J. Cancer Res. Clin. Oncol. 147 (2021) 2507–2534, https://doi.org/10.1007/S00432-021-03710-7.
[13] P. Morales, D.P. Hurst, P.H. Reggio, Molecular targets of the Phytocannabinoids: a complex picture, Prog. Chem. Org. Nat. Prod. 103 (2017) 103–131, https://doi.org/10.1007/978-3-319-45541-9_4.
[14] R.M. Vitale, F.A. Iannotti, P. Amodeo, The (poly)pharmacology of Cannabidiol in neurological and neuropsychiatric disorders: molecular mechanisms and targets, Int. J. Mol. Sci. 22 (2021), https://doi.org/10.3390/IJMS22094876.
[15] G. Velasco, C. Sánchez, M. Guzmán, Anticancer mechanisms of cannabinoids, Curr. Oncol. 23 (2016) S23–S32, https://doi.org/10.3747/CO.23.3080.
[16] T. Huang, T. Xu, Y. Wang, Y. Zhou, D. Yu, Z. Wang, L. He, Z. Chen, Y. Zhang, D. Davidson, Y. Dai, C. Hang, X. Liu, C. Yan, Cannabidiol inhibits human glioma by induction of lethal mitophagy through activating TRPV4, Autophagy 17 (2021) 3592–3606, https://doi.org/10.1080/15548627.2021.1885203.
[17] P. Massi, A. Vaccani, S. Ceruti, A. Colombo, M.P. Abbracchio, D. Parolaro, Antitumor effects of cannabidiol, a nonpsychoactive cannabinoid, on human glioma cell lines, J. Pharmacol. Exp. Ther. 308 (2004) 838–845, https://doi.org/10.1124/JPET.103.061002.
[18] A. Ligresti, A.S. Moriello, K. Starowicz, I. Matias, S. Pisanti, L. De Petrocellis, C. Laezza, G. Portella, M. Bifulco, V. Di Marzo, Antitumor activity of plant cannabinoids with emphasis on the effect of cannabidiol on human breast carcinoma, J. Pharmacol. Exp. Ther. 318 (2006) 1375–1387, https://doi.org/10.1124/JPET.106.105247.
[19] E. Singer, J. Judkins, N. Salomonis, L. Matlaf, P. Soteropoulos, S. McAllister, L. Soroceanu, Reactive oxygen species-mediated therapeutic response and resistance in glioblastoma, Cell Death Dis. 6 (2015), https://doi.org/10.1038/CDDIS.2014.566.
[20] L.D. Schurman, D. Lu, D.A. Kendall, A.C. Howlett, A.H. Lichtman, Molecular mechanism and cannabinoid pharmacology, Handb. Exp. Pharmacol. 258 (2020) 323–353, https://doi.org/10.1007/164_2019_298.
[21] M. Formato, G. Crescente, M. Scognamiglio, A. Fiorentino, M.T. Pecoraro, S. Piccolella, M. Catauro, S. Pacifico, (−)-Cannabidiolic acid, a still overlooked bioactive compound: an introductory review and preliminary research, Molecules 25 (2020), https://doi.org/10.3390/MOLECULES25112638.
[22] S. Takeda, S. Okajima, H. Miyoshi, K. Yoshida, Y. Okamoto, T. Okada, T. Amamoto, K. Watanabe, C.J. Omiecinski, H. Aramaki, Cannabidiolic acid, a major cannabinoid in fiber-type cannabis, is an inhibitor of MDA-MB-231 breast cancer cell migration, Toxicol. Lett. 214 (2012) 314–319, https://doi.org/10.1016/j.toxlet.2012.08.029.
[23] J. Farkas, E. Andrassy, The sporostatic effect of cannabidiolic acid, Acta Aliment. Acad. Sci. Hungaricae. 5 (1976) 57–67, https://inis.iaea.org/search/search.aspx?orig_q=RN:8301251.
[24] S. Giacoppo, A. Gugliandolo, O. Trubiani, F. Pollastro, G. Grassi, P. Bramanti, E. Mazzon, Cannabinoid CB2 receptors are involved in the protection of RAW264.7 macrophages against the oxidative stress: an in vitro study, Eur. J. Histochem. 61 (2017) 1–13, https://doi.org/10.4081/EJH.2017.2749.
[25] L.L. Anderson, I.K. Low, S.D. Banister, I.S. McGregor, J.C. Arnold, Pharmacokinetics of Phytocannabinoid acids and anticonvulsant effect of Cannabidiolic acid in a mouse model of Dravet syndrome, J. Nat. Prod. 82 (2019) 3047–3055, https://doi.org/10.1021/ACS.JNATPROD.9B00600.
[26] G. Navarro, K. Varani, A. Lillo, F. Vincenzi, R. Rivas-Santisteban, I. Raïch, I. Reyes-Resina, C. Ferreiro-Vera, P.A. Borea, V. Sánchez de Medina, X. Nadal, R. Franco, Pharmacological data of cannabidiol- and cannabigerol-type phytocannabinoids acting on cannabinoid CB1, CB2 and CB1/CB2 heteromer receptors, Pharmacol. Res. 159 (2020), https://doi.org/10.1016/J.PHRS.2020.104940.
[27] M. Hirao-Suzuki, K. Takayuki, M. Takiguchi, J.M. Peters, S. Takeda, Cannabidiolic acid activates the expression of the PPARβ/δ target genes in MDA-MB-231 cells, Arch. Biochem. Biophys. 731 (2022), https://doi.org/10.1016/J.ABB.2022.109428.
[28] M. Hirao-Suzuki, S. Takeda, T. Koga, M. Takiguchi, A. Toda, Cannabidiolic acid dampens the expression of cyclooxygenase-2 in MDA-MB-231 breast cancer cells: possible implication of the peroxisome proliferator-activated receptor β/δ abrogation, J. Toxicol. Sci. 45 (2020) 227–236, https://doi.org/10.2131/JTS.45.227.
[29] E. D'Aniello, T. Fellous, F.A. Iannotti, A. Gentile, M. Allarà, F. Balestrieri, R. Gray, P. Amodeo, R.M. Vitale, V. Di Marzo, Identification and characterization of phytocannabinoids as novel dual PPARα/γ agonists by a computational and in vitro experimental approach, Biochim. Biophys. Acta Gen. Subj. 2019 (1863) 586–597, https://doi.org/10.1016/J.BBAGEN.2019.01.002.
[30] F. Meissner, J. Geddes-McAlister, M. Mann, M. Bantscheff, The emerging role of mass spectrometry-based proteomics in drug discovery, Nat. Rev. Drug Discov. 21 (2022) 637–654, https://doi.org/10.1038/S41573-022-00409-3.
[31] Y. Gaoni, R. Mechoulam, Y. Gaoni, R. Mechoulam, The isolation and structure of delta-1-tetrahydrocannabinol and other neutral cannabinoids from hashish, J. Am. Chem. Soc. 93 (1971) 217–224, https://doi.org/10.1021/JA00730A036.
[32] Concise synthesis of biologically interesting (±)-Cannabichromene, (±)-Cannabichromenic acid, and (±)-Daurichromenic acid, Bull. Korean Chem. Soc. 26 (2005) 1933–1936, https://doi.org/10.5012/bkcs.2005.26.12.1933.
[33] A. Shevchenko, H. Tomas, J. Havliš, J.V. Olsen, M. Mann, In-gel digestion for mass spectrometric characterization of proteins and proteomes, Nat. Protoc. 1 (2006) 2856–2860, https://doi.org/10.1038/NPROT.2006.468.
[34] D.A. Case, K. Belfon, I.Y. Ben-Shalom, S.R. Brozell, D.S. Cerutti, T.E. Cheatham III, V.W.D. Cruzeiro, T.A. Darden, R.E. Duke, G. Giambasu, M.K. Gilson, H. Gohlke, A. W. Goetz, R. Harris, S. Izadi, S.A. Izmailov, K. Kasavajhala, A. Kovalenko, R. Krasny, T. Kurtzman, T.S. Lee, S. LeGrand, P. Li, C. Lin, J. Liu, T. Luchko, R. Luo, V. Man, K.M. Merz, Y. Miao, O. Mikhailovskii, G. Monard, H. Nguyen, A. Onufriev, F. Pan, S. Pantano, R. Qi, D.R. Roe, A. Roitberg, C. Sagui, S. Schott-Verdugo, J. Shen, C.L. Simmerling, N.R. Skrynnikov, J. Smith, J. Swails, R.C. Walker, J. Wang, L. Wilson, R.M. Wolf, X. Wu, Y. Xiong, Y. Xue, D.M. York, P.A. Kollman, AMBER 2020, University of California, San Francisco, 2020.
[35] E.F. Pettersen, T.D. Goddard, C.C. Huang, G.S. Couch, D.M. Greenblatt, E.C. Meng, T.E. Ferrin, UCSF Chimera–a visualization system for exploratory research and analysis, J. Comput. Chem. 25 (2004) 1605–1612, https://doi.org/10.1002/JCC.20084.
[36] M.W. Schmidt, K.K. Baldridge, J.A. Boatz, S.T. Elbert, M.S. Gordon, J.H. Jensen, S. Koseki, N. Matsunaga, K.A. Nguyen, S. Su, T.L. Windus, M. Dupuis, J. A. Montgomery, General atomic and molecular electronic structure system, J. Comput. Chem. 14 (1993) 1347–1363, https://doi.org/10.1002/JCC.540141112.
[37] T. Fox, P.A. Kollman, Application of the RESP methodology in the parametrization of organic solvents, J. Phys. Chem. B 102 (1998) 8070–8079, https://doi.org/10.1021/JP9717655.
[38] G.M. Morris, H. Ruth, W. Lindstrom, M.F. Sanner, R.K. Belew, D.S. Goodsell, A. J. Olson, AutoDock4 and AutoDockTools4: automated docking with selective receptor flexibility, J. Comput. Chem. 30 (2009) 2785–2791, https://doi.org/10.1002/JCC.21256.
[39] S.X. Ge, D. Jung, D. Jung, R. Yao, ShinyGO: a graphical gene-set enrichment tool for animals and plants, Bioinformatics 36 (2020) 2628–2629, https://doi.org/10.1093/BIOINFORMATICS/BTZ931.
[40] A. Sainz-Cort, C. Müller-Sánchez, E. Espel, Anti-proliferative and cytotoxic effect of cannabidiol on human cancer cell lines in presence of serum, BMC. Res. Notes 13 (2020), https://doi.org/10.1186/S13104-020-05229-5.
[41] S.O.P. Jacobsson, E. Rongård, M. Stridh, G. Tiger, C.J. Fowler, Serum-dependent effects of tamoxifen and cannabinoids upon C6 glioma cell viability, Biochem. Pharmacol. 60 (2000) 1807–1813, https://doi.org/10.1016/S0006-2952(00)00492-5.
[42] B. Lomenick, R. Hao, N. Jonai, R.M. Chin, M. Aghajan, S. Warburton, J. Wang, R. P. Wu, F. Gomez, J.A. Loo, J.A. Wohlschlegel, T.M. Vondriska, J. Pelletier, H. R. Herschman, J. Clardy, C.F. Clarke, J. Huang, Target identification using drug affinity responsive target stability (DARTS), Proc. Natl. Acad. Sci. U. S. A. 106 (2009) 21984–21989, https://doi.org/10.1073/PNAS.0910040106.
[43] A.A. Komar, W.C. Merrick, A retrospective on eIF2A-and not the alpha subunit of eIF2, Int. J. Mol. Sci. 21 (2020), https://doi.org/10.3390/IJMS21062054.
[44] T.V. Pestova, V.G. Kolupaeva, I.B. Lomakin, E.V. Pilipenko, I.N. Shatsky, V.I. Agol, C.U.T. Hellen, Molecular mechanisms of translation initiation in eukaryotes, Proc. Natl. Acad. Sci. U. S. A. 98 (2001) 7029–7036, https://doi.org/10.1073/PNAS.111145798.
[45] C.E. Aitken, J.R. Lorsch, A mechanistic overview of translation initiation in eukaryotes, Nat. Struct. Mol. Biol. 19 (2012) 568–576, https://doi.org/10.1038/NSMB.2303.
[46] C. Echeverry, G. Prunell, C. Narbondo, V.S. de Medina, X. Nadal, M. Reyes-Parada, C. Scorza, A comparative in vitro study of the neuroprotective effect induced by Cannabidiol, Cannabigerol, and their respective acid forms: relevance of the 5-HT1A receptors, Neurotox. Res. 39 (2021) 335–348, https://doi.org/10.1007/S12640-020-00277-Y.
[47] M.L. Bellone, L. Fiengo, C. Cerchia, R. Cotugno, A. Bader, A. Lavecchia, N. De Tommasi, F.D. Piaz, Impairment of Nucleolin activity and phosphorylation by a Trachylobane Diterpene from Psiadia punctulata in Cancer cells, Int. J. Mol. Sci. 23 (2022), https://doi.org/10.3390/IJMS231911390.
[48] S. Schopper, A. Kahraman, P. Leuenberger, Y. Feng, I. Piazza, O. Müller, P. J. Boersema, P. Picotti, Measuring protein structural changes on a proteome-wide scale using limited proteolysis-coupled mass spectrometry, Nat. Protoc. 12 (2017) 2391–2410, https://doi.org/10.1038/NPROT.2017.100.
[49] E. Kim, J.H. Kim, K. Seo, K.Y. Hong, S.W.A. An, J. Kwon, S.J.V. Lee, S.K. Jang, eIF2A, an initiator tRNA carrier refractory to eIF2α kinases, functions synergistically with eIF5B, Cell. Mol. Life Sci. 75 (2018) 4287–4300, https://doi.org/10.1007/S00018-018-2870-4.

[50] L.C. Reineke, Y. Cao, D. Baus, N.M. Hossain, W.C. Merrick, Insights into the role of yeast eIF2A in IRES-mediated translation, PloS One 6 (2011), https://doi.org/10.1371/JOURNAL.PONE.0024492.
[51] D.J. Grove, D.J. Levine, M.G. Kearse, Increased levels of eIF2A inhibit translation by sequestering 40S ribosomal subunits, Nucleic Acids Res. 51 (2023) 9983–10000, https://doi.org/10.1093/NAR/GKAD683.
[52] K. Eichelbaum, J. Krijgsveld, Combining pulsed SILAC labeling and click-chemistry for quantitative secretome analysis, Methods Mol. Biol. 1174 (2014) 101–114, https://doi.org/10.1007/978-1-4939-0944-5_7/COVER.
[53] T.M. Nthiga, B. Kumar Shrestha, E. Sjøttem, J. Bruun, K. Bowitz Larsen, Z. Bhujabal, T. Lamark, T. Johansen, CALCOCO1 acts with VAMP-associated proteins to mediate ER-phagy, EMBO J. 39 (2020), https://doi.org/10.15252/EMBJ.2019103649.
[54] C.P. Hinzman, B. Singh, S. Bansal, Y. Li, A. Iliuk, M. Girgis, K.M. Herremans, J. G. Trevino, V.K. Singh, P.P. Banerjee, A.K. Cheema, A multi-omics approach identifies pancreatic cancer cell extracellular vesicles as mediators of the unfolded protein response in normal pancreatic epithelial cells, J. Extracell. Vesicles. 11 (2022), https://doi.org/10.1002/JEV2.12232.
[55] G.G. Tall, M.A. Barbieri, P.D. Stahl, B.F. Horazdovsky, Ras-activated endocytosis is mediated by the Rab5 guanine nucleotide exchange activity of RIN1, Dev. Cell 1 (2001) 73–82, https://doi.org/10.1016/S1534-5807(01)00008-9.
[56] M. Mari, M.V. Bujny, D. Zeuschner, W.J.C. Geerts, J. Griffith, C.M. Petersen, P. J. Cullen, J. Klumperman, H.J. Geuze, SNX1 defines an early endosomal recycling exit for sortilin and mannose 6-phosphate receptors, Traffic 9 (2008) 380–393, https://doi.org/10.1111/J.1600-0854.2007.00686.X.
[57] T. Wang, N.S. Liu, L.F. Seet, W. Hong, The emerging role of VHS domain-containing Tom1, Tom1L1 and Tom1L2 in membrane trafficking, Traffic 11 (2010) 1119–1128, https://doi.org/10.1111/J.1600-0854.2010.01098.X.
[58] M.E. Coulter, D. Musaev, E.M. DeGennaro, X. Zhang, K. Henke, K.N. James, R. S. Smith, R.S. Hill, J.N. Partlow, M. Al-Saffar, A.S. Kamumbu, N. Hatem, A. J. Barkovich, J. Aziza, N. Chassaing, M.S. Zaki, T. Sultan, L. Burglen, A. Rajab, L. Al-Gazali, G.H. Mochida, M.P. Harris, J.G. Gleeson, C.A. Walsh, Regulation of human cerebral cortical development by EXOC7 and EXOC8, components of the exocyst complex, and roles in neural progenitor cell proliferation and survival, Genet. Med. 22 (2020) 1040–1050, https://doi.org/10.1038/S41436-020-0758-9.
[59] C.H.H. Hor, B.L. Tang, E.L.K. Goh, Rab23 and developmental disorders, Rev. Neurosci. 29 (2018) 849–860, https://doi.org/10.1515/REVNEURO-2017-0110.
[60] V. Cohen-Kaplan, I. Livneh, N. Avni, C. Cohen-Rosenzweig, A. Ciechanover, The ubiquitin-proteasome system and autophagy: coordinated and independent activities, Int. J. Biochem. Cell Biol. 79 (2016) 403–418, https://doi.org/10.1016/J.BIOCEL.2016.07.019.
[61] Z. Qi, L. Chen, Endoplasmic reticulum stress and autophagy, Adv. Exp. Med. Biol. 1206 (2019) 167–177, https://doi.org/10.1007/978-981-15-0602-4_8.
[62] D.J. Klionsky, A.K. Abdel-Aziz, S. Abdelfatah, M. Abdellatif, A. Abdoli, S. Abel, H. Abeliovich, M.H. Abildgaard, Y.P. Abudu, A. Acevedo-Arozena, I.E. Adamopoulos, K. Adeli, T.E. Adolph, A. Adornetto, E. Aflaki, G. Agam, A. Agarwal, B.B. Aggarwal, M. Agnello, P. Agostinis, J.N. Agrewala, A. Agrotis, P. V. Aguilar, S.T. Ahmad, Z.M. Ahmed, U. Ahumada-Castro, S. Aits, S. Aizawa, Y. Akkoc, T. Akoumianaki, H.A. Akpinar, A.M. Al-Abd, L. Al-Akra, A. Al-Gharaibeh, M.A. Alaoui-Jamali, S. Alberti, E. Alcocer-Gómez, C. Alessandri, M. Ali, M.A. Alim Al-Bari, S. Aliwaini, J. Alizadeh, E. Almacellas, A. Almasan, A. Alonso, G.D. Alonso, N. Altan-Bonnet, D.C. Altieri, É. M.C. Álvarez, S. Alves, C. da Alves Costa, M.M. Alzaharna, M. Amadio, C. Amantini, C. Amaral, S. Ambrosio, A.O. Amer, V. Ammanathan, Z. An, S.U. Andersen, S.A. Andrabi, M. Andrade-Silva, A.M. Andres, S. Angelini, D. Ann, U.C. Anozie, M.Y. Ansari, P. Antas, A. Antebi, Z. Antón, T. Anwar, L. Apetoh, N. Apostolova, T. Araki, Y. Araki, K. Arasaki, W.L. Araújo, J. Araya, C. Arden, M.A. Arévalo, S. Arguelles, E. Arias, J. Arikkath, H. Arimoto, A.R. Ariosa, D. Armstrong-James, L. Arnauné-Pelloquin, A. Aroca, D.S. Arroyo, I. Arsov, R. Artero, D.M.L. Asaro, M. Aschner, M. Ashrafizadeh, O. Ashur-Fabian, A.G. Atanasov, A.K. Au, P. Auberger, H.W. Auner, L. Aurelian, R. Autelli, L. Avagliano, Y. Ávalos, S. Aveic, C. A. Aveleira, T. Avin-Wittenberg, Y. Aydin, S. Ayton, S. Ayyadevara, M. Azzopardi, M. Baba, J.M. Backer, S.K. Backues, D.H. Bae, O.N. Bae, S.H. Bae, E.H. Baehrecke, A. Baek, S.H. Baek, S.H. Baek, G. Bagetta, A. Bagniewska-Zadworna, H. Bai, J. Bai, X. Bai, Y. Bai, N. Bairagi, S. Baksi, T. Balbi, C.T. Baldari, W. Balduini, A. Ballabio, M. Ballester, S. Balazadeh, R. Balzan, R. Bandopadhyay, S. Banerjee, S. Banerjee, Á. Bánréti, Y. Bao, M.S. Baptista, A. Baracca, C. Barbati, A. Bargiela, D. Barilà, P.G. Barlow, S.J. Barmada, E. Barreiro, G.E. Barreto, J. Bartek, B. Bartel, A. Bartolome, G.R. Barve, S.H. Basagoudanavar, D.C. Bassham, R.C. Bast, A. Basu, H. Batoko, I. Batten, E.E. Baulieu, B.L. Baumgarner, J. Bayry, R. Beale, I. Beau, F. Beaumatin, L. R.G. Bechara, G.R. Beck, M.F. Beers, J. Begun, C. Behrends, G.M.N. Behrens, R. Bei, E. Bejarano, S. Bel, C. Behl, A. Belaid, N. Belgareh-Touzé, C. Bellarosa, F. Belleudi, M. Belló Pérez, R. Bello-Morales, J.S.O. de Beltran, S. Beltran, D.M. Benbrook, M. Bendorius, B.A. Benitez, I. Benito-Cuesta, J. Bensalem, M.W. Berchtold, S. Berezowska, D. Bergamaschi, M. Bergami, A. Bergmann, L. Berliocchi, C. Berlioz-Torrent, A. Bernard, L. Berthoux, C.G. Besirli, S. Besteiro, V.M. Betin, R. Beyaert, J. S. Bezbradica, K. Bhaskar, I. Bhatia-Kissova, R. Bhattacharya, S. Bhattacharya, S. Bhattacharyya, M.S. Bhuiyan, S.K. Bhutia, L. Bi, X. Bi, T.J. Biden, K. Bijian, V.A. Billes, N. Binart, C. Bincoletto, A.B. Birgisdottir, G. Bjorkoy, G. Blanco, A. Blas-Garcia, J. Blasiak, R. Blomgran, K. Blomgren, J.S. Blum, E. Boada-Romero, M. Boban, K. Boesze-Battaglia, P. Boeuf, B. Boland, P. Bomont, P. Bonaldo, S.R. Bonam, L. Bonfili, J.S. Bonifacino, B.A. Boone, M.D. Bootman, M. Bordi, C. Borner, B.C. Bornhauser, G. Borthakur, J. Bosch, S. Bose, L.M. Botana, J. Botas, C.M. Boulanger, M.E. Boulton, M. Bourdenx, B. Bourgeois, N.M. Bourke, G. Bousquet, P. Boya, P. V. Bozhkov, L.H.M. Bozi, T.O. Bozkurt, D.E. Brackney, C.H. Brandts, R.J. Braun, G.H. Braus, R. Bravo-Sagua, J.M. Bravo-San Pedro, P. Brest, M.A. Bringer, A. Briones-Herrera, V.C. Broaddus, P. Brodersen, J.L. Brodsky, S.L. Brody, P.G. Bronson, J.M. Bronstein, C.N. Brown, R.E. Brown, P.C. Brum, J.H. Brumell, N. Brunetti-Pierri, D. Bruno, R.J. Bryson-Richardson, C. Bucci, C. Buchrieser, M. Bueno, L.E. Buitrago-Molina, S. Buraschi, S. Buch, J.R. Buchan, E.M. Buckingham, H. Budak, M. Budini, G. Bultynck, F. Burada, J.R. Burgoyne, M.I. Burón, V. Bustos, S. Büttner, E. Butturini, A. Byrd, I. Cabas, S. Cabrera-Benitez, K. Cadwell, J. Cai, L. Cai, Q. Cai, M. Cairó, J.A. Calbet, G.A. Caldwell, K.A. Caldwell, J.A. Call, R. Calvani, A.C. Calvo, M. Calvo-Rubio Barrera, N.O.S. Camara, J.H. Camonis, N. Camougrand, M. Campanella, E.M. Campbell, F.X. Campbell-Valois, S. Campello, I. Campesi, J.C. Campos, O. Camuzard, J. Cancino, D. Candido de Almeida, L. Canesi, I. Caniggia, B. Canonico, C. Cantí, B. Cao, M. Caraglia, B. Caramés, E.H. Carchman, E. Cardenal-Muñoz, C. Cardenas, L. Cardenas, S.M. Cardoso, J.S. Carew, G.F. Carle, G. Carleton, S. Carloni, D. Carmona-Gutierrez, L.A. Carneiro, O. Carnevali, J.M. Carosi, S. Carra, A. Carrier, L. Carrier, B. Carroll, A.B. Carter, A.N. Carvalho, M. Casanova, C. Casas, J. Casas, C. Cassioli, E.F. Castillo, K. Castillo, S. Castillo-Lluva, F. Castoldi, M. Castori, A.F. Castro, M. Castro-Caldas, J. Castro-Hernandez, S. Castro-Obregon, S.D. Catz, C. Cavadas, F. Cavaliere, G. Cavallini, M. Cavinato, M.L. Cayuela, P. Cebollada Rica, V. Cecarini, F. Cecconi, M. Cechowska-Pasko, S. Cenci, V. Ceperuelo-Mallafré, J.J. Cerqueira, J.M. Cerutti, D. Cervia, V.B. Cetintas, S. Cetrullo, H.J. Chae, A.S. Chagin, C.Y. Chai, G. Chakrabarti, O. Chakrabarti, T. Chakraborty, T. Chakraborty, M. Chami, G. Chamilos, D.W. Chan, E.Y.W. Chan, E. D. Chan, H.Y.E. Chan, H.H. Chan, H. Chan, M.T.V. Chan, Y.S. Chan, P.K. Chandra, C.P. Chang, C. Chang, H.C. Chang, K. Chang, J. Chao, T. Chapman, N. Charlet-Berguerand, S. Chatterjee, S.K. Chaube, A. Chaudhary, S. Chauhan, E. Chaum, F. Checler, M.E. Cheetham, C.S. Chen, G.C. Chen, J.F. Chen, L.L. Chen, L. Chen, L. Chen, M. Chen, M.K. Chen, N. Chen, Q. Chen, R.H. Chen, S. Chen, W. Chen, W. Chen, X.M. Chen, X.W. Chen, X. Chen, Y. Chen, Y.G. Chen, Y. Chen, Y. Chen, Y.J., Y.Q. Chen, Z.S. Chen, Z. Chen, Z.H. Chen, Z.J. Chen, Z. Chen, H. Cheng, J. Cheng, S. Y. Cheng, W. Cheng, X. Cheng, X.T. Cheng, Y. Cheng, Z. Cheng, Z. Chen, H. Cheong, J.K. Cheong, B. V. Chernyak, S. Cherry, C.F.R. Cheung, C.H.A. Cheung, K. H. Cheung, E. Chevet, R.J. Chi, A.K.S. Chiang, F. Chiaradonna, R. Chiarelli, M. Chiariello, N. Chica, S. Chiocca, M. Chiong, S.H. Chiou, A.I. Chiramel, V. Chiurchiù, D.H. Cho, S.K. Choe, A.M.K. Choi, M.E. Choi, K.R. Choudhury, N.S. Chow, C.T. Chu, J.P. Chua, J.J.E. Chua, H. Chung, K.P. Chung, S. Chung, S.H. Chung, Y.L. Chung, V. Cianfanelli, I.A. Ciechomska, M. Cifuentes, L. Cinque, S. Cirak, M. Cirone, M.J. Clague, R. Clarke, E. Clementi, E.M. Coccia, P. Codogno, E. Cohen, M.M. Cohen, T. Colasanti, F. Colasuonno, R.A. Colbert, A. Colell, M. Čolić, N.S. Coll, M.O. Collins, M.I. Colombo, D.A. Colón-Ramos, L. Combaret, S. Comincini, M.R. Cominetti, A. Consiglio, A. Conte, F. Conti, V.R. Contu, M.R. Cookson, K.M. Coombs, I. Coppens, M.T. Corasaniti, D.P. Corkery, N. Cordes, K. Cortese, M. C. do Costa, S. Costantino, P. Costelli, A. Coto-Montes, P.J. Crack, J.L. Crespo, A. Criollo, V. Crippa, R. Cristofani, T. Csizmadia, A. Cuadrado, B. Cui, J. Cui, Y. Cui, Y. Cui, E. Culetto, A.C. Cumino, A. V. Cybulsky, M.J. Czaja, S.J. Czuczwar, S. D'Adamo, M. D'Amelio, D. D'Arcangelo, A.C. D'Lugos, G. D'Orazi, J. A. da Silva, H.S. Dafsari, R.K. Dagda, Y. Dagdas, M. Daglia, X. Dai, Y. Dai, Y. Dai, J. Dal Col, P. Dalhaimer, L. Dalla Valle, T. Dallenga, G. Dalmasso, M. Damme, I. Dando, N.P. Dantuma, A.L. Darling, H. Das, S. Dasarathy, S.K. Dasari, S. Dash, O. Daumke, A.N. Dauphinee, J.S. Davies, V.A. Dávila, R.J. Davis, T. Davis, S. Dayalan Naidu, F. De Amicis, K. De Bosscher, F. De Felice, L. De Franceschi, C. De Leonibus, M.G. de Mattos Barbosa, G.R.Y. De Meyer, A. De Milito, C. De Nunzio, C. De Palma, M. De Santi, C. De Virgilio, D. De Zio, J. Debnath, B.J. DeBosch, J.P. Decuypere, M. A. Deehan, G. Deflorian, J. DeGregori, B. Dehay, G. Del Rio, J.R. Delaney, L.M.D. Delbridge, E. Delorme-Axford, M.V. Delpino, F. Demarchi, V. Dembitz, N.D. Demers, H. Deng, Z. Deng, J. Dengjel, P. Dent, D. Denton, M.L. DePamphilis, C.J. Der, V. Deretic, A. Descoteaux, L. Devis, S. Devkota, O. Devuyst, G. Dewson, M. Dharmasivam, R. Dhiman, D. di Bernardo, M. Di Cristina, F. Di Domenico, P. Di Fazio, A. Di Fonzo, G. Di Guardo, G.M. Di Guglielmo, L. Di Leo, C. Di Malta, A. Di Nardo, M. Di Rienzo, F. Di Sano, G. Diallinas, J. Diao, G. Diaz-Araya, I. Díaz-Laviada, J.M. Dickinson, M. Diederich, M. Dieudé, I. Dikic, S. Ding, W.X. Ding, L. Dini, J. Dinić, M. Dinic, A.T. Dinkova-Kostova, M.S. Dionne, J.H.W. Distler, A. Diwan, I.M.C. Dixon, M. Djavaheri-Mergny, I. Dobrinski, O. Dobrovinskaya, R. Dobrowolski, R.C.J. Dobson, J. Đokić, S. Dokmeci Emre, M. Donadelli, B. Dong, X. Dong, Z. Dong, G.W. Dorn, V. Dotsch, H. Dou, J. Dou, M. Dowaidar, S. Dridi, L. Drucker, A. Du, C. Du, G. Du, H.N. Du, L.L. Du, A. du Toit, S. Bin Duan, X. Duan, S. P. Duarte, A. Dubrovska, E.A. Dunlop, N. Dupont, R. V. Durán, B.S. Dwarakanath, S.A. Dyshlovoy, D. Ebrahimi-Fakhari, L. Eckhart, C.L. Edelstein, T. Efferth, E. Eftekharpour, L. Eichinger, N. Eid, T. Eisenberg, N.T. Eissa, S. Eissa, M. Ejarque, A. El Andaloussi, N. El-Hage, S. El-Naggar, A.M. Eleuteri, E.S. El-Shafey, M. Elgendy, A.G. Eliopoulos, M.M. Elizalde, P.M. Elks, H.P. Elsasser, E.S. Elsherbiny, B.M. Emerling, N.C.T. Emre, C.H. Eng, N. Engedal, A.M. Engelbrecht, A.S.T. Engelsen, J. M. Enserink, R. Escalante, A. Esclatine, M. Escobar-Henriques, E.L. Eskelinen, L. Espert, M.O. Eusebio, G. Fabrias, C. Fabrizi, A. Facchiano, F. Facchiano, B. Fadeel, C. Fader, A.C. Faesen, W.D. Fairlie, A. Falcó, B.H. Falkenburger, D. Fan, J. Fan, Y. Fan, E.F. Fang, Y. Fang, Y. Fang, M. Fanto, T. Farfel-Becker, M. Faure, G. Fazeli, A. O. Fedele, A.M. Feldman, D. Feng, J. Feng, L. Feng, Y. Feng, Y. Feng, W. Feng, T. Fenz Araujo, T.A. Ferguson, Á.F. Fernández, J.C. Fernandez-Checa, S. Fernández-Veledo, A.R. Fernie, A.W. Ferrante, A. Ferraresi, M.F. Ferrari, J.C.B. Ferreira, S. Ferro-Novick, A. Figueras, R. Filadi, N. Filigheddu, E. Filippi-Chiela, G. Filomeni, G.M. Fimia, V. Fineschi, F. Finetti, S. Finkbeiner, E.A. Fisher, P.B. Fisher, F. Flamigni, S.J. Fliesler, T.H. Flo, I. Florance, O. Florey, T. Florio, E. Fodor, C. Follo, E.A. Fon, A. Forlino, F. Fornai, P. Fortini, A. Fracassi, A. Fraldi, B. Franco, R. Franco, F. Franconi, L.B. Frankel, S.L. Friedman, L.F. Fröhlich, G. Frühbeck, J.M. Fuentes, Y. Fujiki, N. Fujita, Y. Fujiwara, M. Fukuda, S. Fulda, L. Furic, N. Furuya, C. Fusco, M.U. Gack, L. Gaffke, S. Galadari, A. Galasso, M.F. Galindo, S. Gallolu Kankanamalage, L. Galluzzi, V. Galy, N. Gammoh, B. Gan, I.G. Ganley, F. Gao, H. Gao, M. Gao, P. Gao, S.J. Gao, W. Gao, X. Gao, A. Garcera, M.N. Garcia, V.E. Garcia, F. García-Del Portillo, V. Garcia-Escudero, A. Garcia-Garcia, M. Garcia-

Macia, D. García-Moreno, C. Garcia-Ruiz, P. García-Sanz, A.D. Garg, R. Gargini, T. Garofalo, R.F. Garry, N.C. Gassen, D. Gatica, L. Ge, W. Ge, R. Geiss-Friedlander, C. Gelfi, P. Genschik, I.E. Gentle, V. Gerbino, C. Gerhardt, K. Germain, M. Germain, D. A. Gewirtz, E. Ghasemipour Afshar, S. Ghavami, A. Ghigo, M. Ghosh, G. Giamas, C. Giampietri, A. Giatromanolaki, G.E. Gibson, S.B. Gibson, V. Ginet, E. Giniger, C. Giorgi, H. Girao, S.E. Girardin, M. Giridharan, S. Giuliano, C. Giulivi, S. Giuriato, J. Giustiniani, A. Gluschko, V. Goder, A. Goginashvili, J. Golab, D.C. Goldstone, A. Golebiewska, L.R. Gomes, R. Gomez, R. Gómez-Sánchez, M.C. Gomez-Puerto, R. Gomez-Sintes, Q. Gong, F.M. Goni, J. González-Gallego, T. Gonzalez-Hernandez, R. A. Gonzalez-Polo, J.A. Gonzalez-Reyes, P. González-Rodríguez, I.S. Goping, M.S. Gorbatyuk, N. V. Gorbunov, K. Görgülü, R.M. Gorojod, S.M. Gorski, S. Goruppi, C. Gotor, R.A. Gottlieb, I. Gozes, D. Gozuacik, M. Graef, M.H. Gräler, V. Granatiero, D. Grasso, J.P. Gray, D.R. Green, A. Greenhough, S.L. Gregory, E.F. Griffin, M.W. Grinstaff, F. Gros, C. Grose, A.S. Gross, F. Gruber, P. Grumati, T. Grune, X. Gu, J.L. Guan, C.M. Guardia, K. Guda, F. Guerra, C. Guerri, P. Guha, C. Guillén, S. Gujar, A. Gukovskaya, I. Gukovsky, J. Gunst, A. Günther, A.R. Guntur, C. Guo, C. Guo, H. Guo, L.W. Guo, M. Guo, P. Gupta, S.K. Gupta, S. Gupta, V.B. Gupta, V. Gupta, A.B. Gustafsson, D.D. Gutterman, R. H.B., A. Haapasalo, J.E. Haber, A. Hać, S. Hadano, A.J. Hafrén, M. Haidar, B.S. Hall, G. Halldén, A. Hamacher-Brady, A. Hamann, M. Hamasaki, W. Han, M. Hansen, P.I. Hanson, Z. Hao, M. Harada, L. Harhaji-Trajkovic, N. Hariharan, N. Haroon, J. Harris, T. Hasegawa, N. Hasima Nagoor, J. A. Haspel, V. Haucke, W.D. Hawkins, B.A. Hay, C.M. Haynes, S.B. Hayrabedyan, T. S. Hays, C. He, Q. He, R.R. He, Y.W. He, Y.Y. He, Y. Heakal, A.M. Heberle, J.F. Hejtmancik, G.V. Helgason, V. Henkel, M. Herb, A. Hergovich, A. Herman-Antosiewicz, A. Hernández, C. Hernandez, S. Hernandez-Diaz, V. Hernandez-Gea, A. Herpin, J. Herreros, J.H. Hervás, D. Hesselson, C. Hetz, V.T. Heussler, Y. Higuchi, S. Hilfiker, J.A. Hill, W.S. Hlavacek, E.A. Ho, I.H.T. Ho, P.W.L. Ho, S.L. Ho, W.Y. Ho, G.A. Hobbs, M. Hochstrasser, P.H.M. Hoet, D. Hofius, P. Hofman, A. Höhn, C.I. Holmberg, J.R. Hombrebueno, C.W.H. Yi-Ren Hong, L. V. Hooper, T. Hoppe, R. Horos, Y. Hoshida, I.L. Hsin, H.Y. Hsu, B. Hu, D. Hu, L.F. Hu, M.C. Hu, R. Hu, W. Hu, Y.C. Hu, Z.W. Hu, F. Hua, J. Hua, Y. Hua, C. Huan, C. Huang, C. Huang, C. Huang, C. Huang, H. Huang, K. Huang, M.L.H. Huang, R. Huang, S. Huang, T. Huang, X. Huang, Y.J. Huang, T.B. Huber, V. Hubert, C.A. Hubner, S.M. Hughes, W.E. Hughes, M. Humbert, G. Hummer, J.H. Hurley, S. Hussain, S. Hussain, P.J. Hussey, M. Hutabarat, H.Y. Hwang, S. Hwang, A. Ieni, F. Ikeda, Y. Imagawa, Y. Imai, C. Imbriano, M. Imoto, D.M. Inman, K. Inoki, J. Iovanna, R. V. Iozzo, G. Ippolito, J.E. Irazoqui, P. Iribarren, M. Ishaq, M. Ishikawa, N. Ishimwe, C. Isidoro, N. Ismail, S. Issazadeh-Navikas, E. Itakura, D. Ito, D. Ivankovic, S. Ivanova, A.K. V. Iyer, J.M. Izquierdo, M. Izumi, M. Jäättelä, M.S. Jabir, W.T. Jackson, N. Jacobo-Herrera, A.C. Jacomin, E. Jacquin, P. Jadiya, H. Jaeschke, C. Jagannath, A.J. Jakobi, J. Jakobsson, B. Janji, P. Jansen-Dürr, P.J. Jansson, J. Jantsch, S. Januszewski, A. Jassey, S. Jean, H. Jeltsch-David, P. Jendelova, A. Jenny, T.E. Jensen, N. Jessen, J.L. Jewell, J. Ji, L. Jia, R. Jia, L. Jiang, Q. Jiang, R. Jiang, T. Jiang, X. Jiang, Y. Jiang, M. Jimenez-Sanchez, E.J. Jin, F. Jin, H. Jin, L. Jin, L. Jin, M. Jin, S. Jin, E.K. Jo, C. Joffre, T. Johansen, G.V.W. Johnson, S.A. Johnston, E. Jokitalo, M.K. Jolly, L.A.B. Joosten, J. Jordan, B. Joseph, D. Ju, J.S. Ju, J. Ju, E. Juárez, D. Judith, G. Juhász, Y. Jun, C.H. Jung, S.C. Jung, Y.K. Jung, H. Jungbluth, J. Jungverdorben, S. Just, K. Kaarniranta, A. Kaasik, T. Kabuta, D. Kaganovich, A. Kahana, R. Kain, S. Kajimura, M. Kalamvoki, M. Kalia, D.S. Kalinowski, N. Kaludercic, I. Kalvari, J. Kaminska, V.O. Kaminskyy, H. Kanamori, K. Kanasaki, C. Kang, R. Kang, S.S. Kang, S. Kaniyappan, T. Kanki, T.D. Kanneganti, A.G. Kanthasamy, A. Kanthasamy, M. Kantorow, O. Kapuy, M. V. Karamouzis, M.R. Karim, P. Karmakar, R.G. Katare, M. Kato, S.H.E. Kaufmann, A. Kauppinen, G.P. Kaushal, S. Kaushik, K. Kawasaki, K. Kazan, P.Y. Ke, D.J. Keating, U. Keber, J.H. Kehrl, K.E. Keller, C.W. Keller, J.K. Kemper, C.M. Kenific, O. Kepp, S. Kermorgant, A. Kern, R. Ketteler, T.G. Keulers, B. Khalfin, H. Khalil, B. Khambu, S.Y. Khan, V.K. M. Khandelwal, R. Khandia, W. Kho, N. V. Khobrekar, S. Khuansuwan, M. Khundadze, S.A. Killackey, D. Kim, D.R. Kim, D.H. Kim, D.E. Kim, E.Y. Kim, E.K. Kim, H.R. Kim, H.S. Kim, Hyung-Ryong Kim, J.H. Kim, J.K. Kim, J.H. Kim, J. Kim, J.H. Kim, K. Il Kim, P.K. Kim, S.J. Kim, S.R. Kimball, A. Kimchi, A.C. Kimmelman, T. Kimura, M.A. King, K.J. Kinghorn, C.G. Kinsey, V. Kirkin, L.A. Kirshenbaum, S.L. Kiselev, S. Kishi, K. Kitamoto, Y. Kitaoka, K. Kitazato, R.N. Kitsis, J.T. Kittler, O. Kjaerulff, P.S. Klein, T. Klopstock, J. Klucken, H. Knævelsrud, R.L. Knorr, B.C.B. Ko, F. Ko, J.L. Ko, H. Kobayashi, S. Kobayashi, I. Koch, J.C. Koch, U. Koenig, D. Kögel, Y.H. Koh, M. Koike, S.D. Kohlwein, N.M. Kocaturk, M. Komatsu, J. König, T. Kono, B.T. Kopp, T. Korcsmaros, G. Korkmaz, V.I. Korolchuk, M.S. Korsnes, A. Koskela, J. Kota, Y. Kotake, M.L. Kotler, Y. Kou, M.I. Koukourakis, E. Koustas, A.L. Kovacs, T. Kovács, D. Koya, T. Kozako, C. Kraft, D. Krainc, H. Krämer, A.D. Krasnodembskaya, C. Kretz-Remy, G. Kroemer, N.T. Ktistakis, K. Kuchitsu, S. Kuenen, L. Kuerschner, T. Kukar, A. Kumar, A. Kumar, D. Kumar, D. Kumar, S. Kumar, S. Kume, C. Kumsta, C.N. Kundu, M. Kundu, A.B. Kunnumakkara, L. Kurgan, T.G. Kutateladze, O. Kutlu, S.A. Kwak, H.J. Kwon, T.K. Kwon, Y.T. Kwon, I. Kyrmizi, A. La Spada, P. Labonté, S. Ladoire, I. Laface, F. Lafont, D.C. Lagace, V. Lahiri, Z. Lai, A.S. Laird, A. Lakkaraju, T. Lamark, S.H. Lan, A. Landajuela, D.J.R. Lane, J.D. Lane, C.H. Lang, C. Lange, Ü. Langel, R. Langer, P. Lapaquette, J. Laporte, N.F. LaRusso, I. Lastres-Becker, W.C.Y. Lau, G.W. Laurie, S. Lavandero, B.Y.K. Law, H.K. Wai Law, R. Layfield, W. Le, H. Le Stunff, A.Y. Leary, J.J. Lebrun, L.Y.W. Leck, J.P. Leduc-Gaudet, C. Lee, C.P. Lee, D.H. Lee, E.B. Lee, E.F. Lee, G.M. Lee, H.J. Lee, H.K. Lee, J. M. Lee, J.S. Lee, J.A. Lee, J.Y. Lee, J.H. Lee, M. Lee, M.G. Lee, M.J. Lee, M.S. Lee, S. Y. Lee, S.J. Lee, S.Y. Lee, S.B. Lee, W.H. Lee, Y.R. Lee, Y. Ho Lee, Y. Lee, C. Lefebvre, R. Legouis, Y.L. Lei, Y. Lei, S. Leikin, G. Leitinger, L. Lemus, S. Leng, O. Lenoir, G. Lenz, H.J. Lenz, P. Lenzi, Y. León, A.M. Leopoldino, C. Leschczyk, S. Leskelä, E. Letellier, C.T. Leung, P.S. Leung, J.S. Leventhal, B. Levine, P.A. Lewis, K. Ley, B. Li, D.Q. Li, J. Li, J. Li, J. Li, K. Li, L. Li, M. Li, M. Li, M. Li, M. Li, M. Li, P.L. Li, M.Q. Li, Q. Li, S. Li, T. Li, W. Li, W. Li, X. Li, Y.P. Li, Y. Li, Z. Li, Z. Li, Z. Li, J. Lian, C. Liang, Q. Liang, W. Liang, Y. Liang, Y.T. Liang, G. Liao, L. Liao, M. Liao, Y. F. Liao, M. Librizzi, P.P.Y. Lie, M.A. Lilly, H.J. Lim, T.R.R. Lima, F. Limana, C. Lin, C.W. Lin, D.S. Lin, F.C. Lin, J.D. Lin, K.M. Lin, K.H. Lin, L.T. Lin, P.H. Lin, Q. Lin, S. Lin, S.J. Lin, W. Lin, X. Lin, Y.X. Lin, Y.S. Lin, R. Linden, P. Lindner, S.C. Ling, P. Lingor, A.K. Linnemann, Y.C. Liou, M.M. Lipinski, S. Lipovšek, V.A. Lira, N. Lisiak, P.B. Liton, C. Liu, C.H. Liu, C.F. Liu, C.H. Liu, F. Liu, H. Liu, H.S. Liu, H. Feng Liu, H. Liu, J. Liu, J. Liu, J. Liu, L. Liu, L. Liu, M. Liu, Q. Liu, W. Liu, W. Liu, X.H. Liu, X. Liu, X. Liu, X. Liu, Y. Liu, Y. Liu, Y. Liu, Y. Liu, Y. Liu, J.A. Livingston, G. Lizard, J.M. Lizcano, S. Ljubojevic-Holzer, M.E. LLeonart, D. Llobet-Navàs, A. Llorente, C.H. Lo, D. Lobato-Márquez, Q. Long, Y.C. Long, B. Loos, J.A. Loos, M.G. López, G. López-Doménech, J.A. López-Guerrero, A.T. López-Jiménez, Ó. López-Pérez, I. López-Valero, M.J. Lorenowicz, M. Lorente, P. Lorincz, L. Lossi, S. Lotersztajn, P.E. Lovat, J.F. Lovell, A. Lovy, P. Lőw, G. Lu, H. Lu, J.H. Lu, J.J. Lu, M. Lu, S. Lu, A. Luciani, J.M. Lucocq, P. Ludovico, M.A. Luftig, M. Luhr, D. Luis-Ravelo, J.J. Lum, L. Luna-Dulcey, A.H. Lund, V.K. Lund, J.D. Lünemann, P. Lüningschrör, H. Luo, R. Luo, S. Luo, Z. Luo, C. Luparello, B. Lüscher, L. Luu, A. Lyakhovich, K.G. Lyamzaev, A.H. Lystad, L. Lytvynchuk, A.C. Ma, C. Ma, M. Ma, N. F. Ma, Q.H. Ma, X. Ma, Y. Ma, Z. Ma, O.A. MacDougald, F. Macian, G.C. MacIntosh, J.P. MacKeigan, K.F. Macleod, S. Maday, F. Madeo, M. Madesh, T. Madl, J. Madrigal-Matute, A. Maeda, Y. Maejima, M. Magarinos, P. Mahavadi, E. Maiani, K. Maiese, P. Maiti, M.C. Maiuri, B. Majello, M.B. Major, E. Makareeva, F. Malik, K. Mallilankaraman, W. Malorni, A. Maloyan, N. Mammadova, G.C.W. Man, F. Manai, J.D. Mancias, E.M. Mandelkow, M.A. Mandell, A.A. Manfredi, M.H. Manjili, R. Manjithaya, P. Manque, B.B. Manshian, R. Manzano, C. Manzoni, K. Mao, C. Marchese, S. Marchetti, A.M. Marconi, F. Marcucci, S. Mardente, O.A. Mareninova, M. Margeta, M. Mari, S. Marinelli, O. Marinelli, G. Mariño, S. Mariotto, R.S. Marshall, M.R. Marten, S. Martens, A.P.J. Martin, K.R. Martin, S. Martin, S. Martin, A. Martín-Segura, M.A. Martín-Acebes, I. Martin-Burriel, M. Martin-Rincon, P. Martin-Sanz, J.A. Martina, W. Martinet, A. Martinez, A. Martinez, J. Martinez, M. Martinez Velazquez, N. Martinez-Lopez, M. Martinez-Vicente, D.O. Martins, J.O. Martins, W.K. Martins, T. Martins-Marques, E. Marzetti, S. Masaldan, C. Masclaux-Daubresse, D.G. Mashek, V. Massa, L. Massieu, G.R. Masson, L. Masuelli, A.I. Masyuk, T. V. Masyuk, P. Matarrese, A. Matheu, S. Matoba, S. Matsuzaki, P. Mattar, A. Matte, D. Mattoscio, J.L. Mauriz, M. Mauthe, C. Mauvezin, E. Maverakis, P. Maycotte, J. Mayer, G. Mazzoccoli, C. Mazzoni, J.R. Mazzulli, N. McCarty, C. McDonald, M.R. McGill, S.L. McKenna, B.A. McLaughlin, F. McLoughlin, M.A. McNiven, T.G. McWilliams, F. Mechta-Grigoriou, T.C. Medeiros, D.L. Medina, L.A. Megeney, K. Megyeri, M. Mehrpour, J.L. Mehta, A.J. Meijer, A.H. Meijer, J. Mejlvang, A. Meléndez, A. Melk, G. Memisoglu, A.F. Mendes, D. Meng, F. Meng, T. Meng, R. Menna-Barreto, M.B. Menon, C. Mercer, A.E. Mercier, J.L. Mergny, A. Merighi, S.D. Merkley, G. Merla, V. Meske, A.C. Mestre, S.P. Metur, C. Meyer, H. Meyer, W. Mi, J. Mialet-Perez, J. Miao, L. Micale, Y. Miki, E. Milan, M. Milczarek, D.L. Miller, S.I. Miller, S. Miller, S.W. Millward, I. Milosevic, E.A. Minina, H. Mirzaei, H.R. Mirzaei, M. Mirzaei, A. Mishra, N. Mishra, P.K. Mishra, M. Misirkic Marjanovic, R. Misasi, A. Misra, G. Misso, C. Mitchell, G. Mitou, T. Miura, S. Miyamoto, M. Miyazaki, M. Miyazaki, T. Miyazaki, K. Miyazawa, N. Mizushima, T. H. Mogensen, B. Mograbi, R. Mohammadinejad, Y. Mohamud, A. Mohanty, S. Mohapatra, T. Möhlmann, A. Mohmmed, A. Moles, K.H. Moley, M. Molinari, V. Mollace, A.B. Møller, B. Mollereau, F. Mollinedo, C. Montagna, M.J. Monteiro, A. Montella, L.R. Montes, B. Montico, V.K. Mony, G. Monzio Compagnoni, M.N. Moore, M.A. Moosavi, A.L. Mora, M. Mora, D. Morales-Alamo, R. Moratalla, P.I. Moreira, E. Morelli, S. Moreno, D. Moreno-Blas, V. Moresi, B. Morga, A.H. Morgan, F. Morin, H. Morishita, O.L. Moritz, M. Moriyama, Y. Moriyasu, M. Morleo, E. Morselli, J.F. Moruno-Manchon, J. Moscat, S. Mostowy, E. Motori, A.F. Moura, N. Moustaid-Moussa, M. Mrakovcic, G. Muciño-Hernández, A. Mukherjee, S. Mukhopadhyay, J.M. Mulcahy Levy, V. Mulero, S. Muller, C. Münch, A. Munjal, P. Munoz-Canoves, T. Muñoz-Galdeano, C. Münz, T. Murakawa, C. Muratori, B.M. Murphy, J.P. Murphy, A. Murthy, T.T. Myöhänen, I.U. Mysorekar, J. Mytych, S.M. Nabavi, M. Nabissi, P. Nagy, J. Nah, A. Nahimana, I. Nakagawa, K. Nakamura, H. Nakatogawa, S.S. Nandi, M. Nanjundan, M. Nanni, G. Napolitano, R. Nardacci, M. Narita, M. Nassif, I. Nathan, M. Natsumeda, R.J. Naude, C. Naumann, O. Naveiras, F. Navid, S.T. Nawrocki, T.Y. Nazarko, F. Nazio, F. Negoita, T. Neill, A.L. Neisch, L. M. Neri, M.G. Netea, P. Neubert, T.P. Neufeld, D. Neumann, A. Neutzner, P.T. Newton, P.A. Ney, I.P. Nezis, C.C.W. Ng, T.B. Ng, H.T.T. Nguyen, L.T. Nguyen, H. M. Ni, C. Ní Cheallaigh, Z. Ni, M.C. Nicolao, F. Nicoli, M. Nieto-Diaz, P. Nilsson, S. Ning, R. Niranjan, H. Nishimune, M. Niso-Santano, R.A. Nixon, A. Nobili, C. Nobrega, T. Noda, U. Nogueira-Recalde, T.M. Nolan, I. Nombela, I. Novak, B. Novoa, T. Nozawa, N. Nukina, C. Nussbaum-Krammer, J. Nylandsted, T.R. O'Donovan, S.M. O'Leary, E.J. O'Rourke, M.P. O'Sullivan, T.E. O'Sullivan, S. Oddo, I. Oehme, M. Ogawa, E. Ogier-Denis, M.H. Ogmundsdottir, B. Ogretmen, G. T. Oh, S.H. Oh, Y.J. Oh, T. Ohama, Y. Ohashi, M. Ohmuraya, V. Oikonomou, R. Ojha, K. Okamoto, H. Okazawa, M. Oku, S. Oliván, J.M.A. Oliveira, M. Ollmann, J. A. Olzmann, S. Omari, M.B. Omary, G. Önal, M. Ondrej, S.B. Ong, S.G. Ong, A. Onnis, J.A. Orellana, S. Orellana-Muñoz, M.D.M. Ortega-Villaizan, X.R. Ortiz-Gonzalez, E. Ortona, H.D. Osiewacz, A.H.K. Osman, R. Osta, M.S. Otegui, K. Otsu, C. Ott, L. Ottobrini, J. Hsiung, J. Ou, T.F. Outeiro, I. Oynebraten, M. Ozturk, G. Pagès, S. Pahari, M. Pajares, U.B. Pajvani, R. Pal, S. Paladino, N. Pallet, M. Palmieri, G. Palmisano, C. Palumbo, F. Pampaloni, L. Pan, Q. Pan, W. Pan, X. Pan, G. Panasyuk, R. Pandey, U.B. Pandey, V. Pandya, F. Paneni, S.Y. Pang, E. Panzarini, D.L. Papademetrio, E. Papaleo, D. Papinski, D. Papp, E.C. Park, H.T. Park, J.M. Park, J.I. Park, J.T. Park, J. Park, S.C. Park, S.Y. Park, A.H. Parola, J.B. Parys, A. Pasquier, B. Pasquier, J.F. Passos, N. Pastore, H.H. Patel, D. Patschan, S. Pattingre, G. Pedraza-Alva, J. Pedraza-Chaverri, Z. Pedrozo, G. Pei, J. Pei, H. Peled-Zehavi, J. M. Pellegrini, J. Pelletier, M.A. Peñalva, D. Peng, Y. Peng, F. Penna, M. Pennuto, F. Pentimalli, C.M.F. Pereira, G.J.S. Pereira, L.C. Pereira, L. Pereira de Almeida, N.D. Perera, Á. Pérez-Lara, A.B. Perez-Oliva, M.E. Pérez-Pérez, P. Periyasamy, A. Perl, C. Perrotta, I. Perrotta, R.G. Pestell, M. Petersen, I. Petrache, G. Petrovski, T.

Pfirrmann, A.S. Pfister, J.A. Philips, H. Pi, A. Picca, A.M. Pickrell, S. Picot, G.M. Pierantoni, M. Pierdominici, P. Pierre, V. Pierrefite-Carle, K. Pierzynowska, F. Pietrocola, M. Pietruczuk, C. Pignata, F.X. Pimentel-Muiños, M. Pinar, R.O. Pinheiro, R. Pinkas-Kramarski, P. Pinton, K. Pircs, S. Piya, P. Pizzo, T.S. Plantinga, H.W. Platta, A. Plaza-Zabala, M. Plomann, E.Y. Plotnikov, H. Plun-Favreau, R. Pluta, R. Pocock, S. Pöggeler, C. Pohl, M. Poirot, A. Poletti, M. Ponpuak, H. Popelka, B. Popova, H. Porta, S. Porte Alcon, E. Portilla-Fernandez, M. Post, M.B. Potts, J. Poulton, T. Powers, V. Prahlad, T.K. Prajsnar, D. Praticò, R. Prencipe, M. Priault, T. Proikas-Cezanne, V.J. Promponas, C.G. Proud, R. Puertollano, L. Puglielli, T. Pulinilkunnil, D. Puri, R. Puri, J. Puyal, X. Qi, Y. Qi, W. Qian, L. Qiang, Y. Qiu, J. Quadrilatero, J. Quarleri, N. Raben, H. Rabinowich, D. Ragona, M.J. Ragusa, N. Rahimi, M. Rahmati, V. Raia, N. Raimundo, N.S. Rajasekaran, S. Ramachandra Rao, A. Rami, I. Ramírez-Pardo, D.B. Ramsden, F. Randow, P.N. Rangarajan, D. Ranieri, H. Rao, L. Rao, R. Rao, S. Rathore, J.A. Ratnayaka, E.A. Ratovitski, P. Ravanan, G. Ravegnini, S.K. Ray, B. Razani, V. Rebecca, F. Reggiori, A. Régnier-Vigouroux, A.S. Reichert, D. Reigada, J.H. Reiling, T. Rein, S. Reipert, R.S. Rekha, H. Ren, J. Ren, W. Ren, T. Renault, G. Renga, K. Reue, K. Rewitz, B. Ribeiro de Andrade Ramos, S.A. Riazuddin, T.M. Ribeiro-Rodrigues, J.E. Ricci, R. Ricci, V. Riccio, D.R. Richardson, Y. Rikihisa, M. V. Risbud, R.M. Risueño, K. Ritis, S. Rizza, R. Rizzuto, H.C. Roberts, L.D. Roberts, K.J. Robinson, M.C. Roccheri, S. Rocchi, G.G. Rodney, T. Rodrigues, V.R. Rodrigues Silva, A. Rodriguez, R. Rodriguez-Barrueco, N. Rodriguez-Henche, H. Rodriguez-Rocha, J. Roelofs, R.S. Rogers, V. V. Rogov, A.I. Rojo, K. Rolka, V. Romanello, L. Romani, A. Romano, P.S. Romano, D. Romeo-Guitart, L.C. Romero, M. Romero, J.C. Roney, C. Rongo, S. Roperto, M.T. Rosenfeldt, P. Rosenstiel, A.G. Rosenwald, K.A. Roth, L. Roth, S. Roth, K.M.A. Rouschop, B.D. Roussel, S. Roux, P. Rovere-Querini, A. Roy, A. Rozieres, D. Ruano, D.C. Rubinsztein, M.P. Rubtsova, K. Ruckdeschel, C. Ruckenstuhl, E. Rudolf, R. Rudolf, A. Ruggieri, A.A. Ruparelia, P. Rusmini, R.R. Russell, G.L. Russo, M. Russo, R. Russo, O.O. Ryabaya, K.M. Ryan, K.Y. Ryu, M. Sabater-Arcis, U. Sachdev, M. Sacher, C. Sachse, A. Sadhu, J. Sadoshima, N. Safren, P. Saftig, A.P. Sagona, G. Sahay, A. Sahebkar, M. Sahin, O. Sahin, S. Sahni, N. Saito, S. Saito, T. Saito, R. Sakai, Y. Sakai, J.I. Sakamaki, K. Saksela, G. Salazar, A. Salazar-Degracia, G.H. Salekdeh, A.K. Saluja, B. Sampaio-Marques, M.C. Sanchez, J.A. Sanchez-Alcazar, V. Sanchez-Vera, V. Sancho-Shimizu, J.T. Sanderson, M. Sandri, S. Santaguida, L. Santambrogio, M.M. Santana, G. Santoni, A. Sanz, P. Sanz, S. Saran, M. Sardiello, T.J. Sargeant, A. Sarin, C. Sarkar, S. Sarkar, M.R. Sarrias, S. Sarkar, D.T. Sarmah, J. Sarparanta, A. Sathyanarayan, R. Sathyanarayanan, K.M. Scaglione, F. Scatozza, L. Schaefer, Z.T. Schafer, U.E. Schaible, A.H.V. Schapira, M. Scharl, H.M. Schatzl, C.H. Schein, W. Scheper, D. Scheuring, M.V. Schiaffino, M. Schiappacassi, R. Schindl, U. Schlattner, O. Schmidt, R. Schmitt, S.D. Schmidt, I. Schmitz, E. Schmukler, A. Schneider, B.E. Schneider, R. Schober, A.C. Schoijet, M. B. Schott, M. Schramm, B. Schröder, K. Schuh, C. Schüller, R.J. Schulze, L. Schürmanns, J.C. Schwamborn, M. Schwarten, F. Scialo, S. Sciarretta, M.J. Scott, K. W. Scotto, A.I. Scovassi, A. Scrima, A. Scrivo, D. Sebastian, S. Sebti, S. Sedej, L. Segatori, N. Segev, P.O. Seglen, I. Seiliez, E. Seki, S.B. Selleck, F.W. Sellke, J.T. Selsby, M. Sendtner, S. Senturk, E. Seranova, C. Sergi, R. Serra-Moreno, H. Sesaki, C. Settembre, S.R.G. Setty, G. Sgarbi, O. Sha, J.J. Shacka, J.A. Shah, D. Shang, C. Shao, F. Shao, S. Sharbati, L.M. Sharkey, D. Sharma, G. Sharma, K. Sharma, P. Sharma, S. Sharma, H.M. Shen, H. Shen, J. Shen, M. Shen, W. Shen, Z. Shen, R. Sheng, Z. Sheng, Z.H. Sheng, J. Shi, X. Shi, Y.H. Shi, K. Shiba-Fukushima, J.J. Shieh, Y. Shimada, S. Shimizu, M. Shimozawa, T. Shintani, C.J. Shoemaker, S. Shojaei, I. Shoji, B. V. Shravage, V. Shridhar, C.W. Shu, H.B. Shu, K. Shui, A.K. Shukla, T.E. Shutt, V. Sica, A. Siddiqui, A. Sierra, V. Sierra-Torre, S. Signorelli, P. Sil, B.J. d. A. Silva, J.D. Silva, E. Silva-Pavez, S. Silvente-Poirot, R.E. Simmonds, A. K. Simon, H.U. Simon, M. Simons, A. Singh, L.P. Singh, R. Singh, S. V. Singh, S.K. Singh, S.B. Singh, S. Singh, S.P. Singh, D. Sinha, R.A. Sinha, S. Sinha, A. Sirko, K. Sirohi, E.L. Sivridis, P. Skendros, A. Skirycz, I. Slaninová, S.S. Smaili, A. Smertenko, M.D. Smith, S.J. Soenen, E.J. Sohn, S.P.M. Sok, G. Solaini, T. Soldati, S.A. Soleimanpour, R.M. Soler, A. Solovchenko, J.A. Somarelli, A. Sonawane, F. Song, H.K. Song, J.X. Song, K. Song, Z. Song, L.R. Soria, M. Sorice, A.A. Soukas, S.F. Soukup, D. Sousa, N. Sousa, P.A. Spagnuolo, S.A. Spector, M.M. Srinivas Bharath, D. St. Clair, V. Stagni, L. Staiano, C.A. Stalnecker, M. V. Stankov, P.B. Stathopulos, K. Stefan, S.M. Stefan, L. Stefanis, J.S. Steffan, A. Steinkasserer, H. Stenmark, J. Sternecker, C. Stevens, V. Stoka, S. Storch, B. Stork, F. Strappazzon, A.M. Strohecker, D.G. Stupack, H. Su, L.Y. Su, L. Su, A.M. Suarez-Fontes, C.S. Subauste, S. Subbian, P. V. Subirada, G. Sudhandiran, C.M. Sue, X. Sui, C. Summers, G. Sun, J. Sun, K. Sun, M. Xiang Sun, Q. Sun, Y. Sun, Z. Sun, K.K.S. Sunahara, E. Sundberg, K. Susztak, P. Sutovsky, H. Suzuki, G. Sweeney, J.D. Symons, S.C.W. Sze, N.J. Szewczyk, A. Tabęcka-Łonczynska, C. Tabolacci, F. Tacke, H. Taegtmeyer, M. Tafani, M. Tagaya, H. Tai, S.W.G. Tait, Y. Takahashi, S. Takats, P. Talwar, C. Tam, S.Y. Tam, D. Tampellini, A. Tamura, C.T. Tan, E.K. Tan, Y.Q. Tan, M. Tanaka, M. Tanaka, D. Tang, J. Tang, T.S. Tang, I. Tanida, Z. Tao, M. Taouis, L. Tatenhorst, N. Tavernarakis, A. Taylor, G.A. Taylor, J.M. Taylor, E. Tchetina, A.R. Tee, I. Tegeder, D. Teis, N. Teixeira, F. Teixeira-Clerc, K.A. Tekirdag, T. Tencomnao, S. Tenreiro, A. V. Tepikin, P.S. Testillano, G. Tettamanti, P.L. Tharaux, K. Thedieck, A.A. Thekkinghat, S. Thellung, J.W. Thinwa, V.P. Thirumalaikumar, S.M. Thomas, P.G. Thomes, A. Thorburn, L. Thukral, T. Thum, M. Thumm, L. Tian, A. Tichy, A. Till, V. Timmerman, V.I. Titorenko, S. V. Todi, K. Todorova, J.M. Toivonen, L. Tomaipitinca, D. Tomar, C. Tomas-Zapico, S. Tomić, B.C.K. Tong, C. Tong, X. Tong, S.A. Tooze, M.L. Torgersen, S. Torii, L. Torres-López, A. Torriglia, C.G. Towers, R. Towns, S. Toyokuni, V. Trajkovic, D. Tramontano, Q.G. Tran, L.H. Travassos, C.B. Trelford, S. Tremel, I.P. Trougakos, B.P. Tsao, M.P. Tschan, H.F. Tse, T.F. Tse, H. Tsugawa, A.S. Tsvetkov, D.A. Tumbarello, Y. Tumtas, M.J. Tuñón, S. Turcotte, B. Turk, V. Turk, B.J. Turner, R.I. Tuxworth, J.K. Tyler, E. V. Tyutereva, Y. Uchiyama, A. Ugun-Klusek, H.H. Uhlig, M. Ułamek-Kozioł, I. V. Ulasov, M. Umekawa, C. Ungermann, R. Unno, S. Urbe, E. Uribe-Carretero, S. Üstün, V.N. Uversky, T. Vaccari, M.I. Vaccaro, B.F. Vahsen, H. Vakifahmetoglu-Norberg, R. Valdor, M.J. Valente, A. Valko, R.B. Vallee, A.M. Valverde, G. Van den Berghe, S. van der Veen, L. Van Kaer, J. van Loosdregt, S.J.L. van Wijk, W. Vandenberghe, I. Vanhorebeek, M.A. Vannier-Santos, N. Vannini, M.C. Vanrell, C. Vantaggiato, G. Varano, I. Varela-Nieto, M. Varga, M.H. Vasconcelos, S. Vats, D.G. Vavvas, I. Vega-Naredo, S. Vega-Rubin-de-Celis, G. Velasco, A.P. Velázquez, T. Vellai, E. Vellenga, F. Velotti, M. Verdier, P. Verginis, I. Vergne, P. Verkade, M. Verma, P. Verstreken, T. Vervliet, J. Vervoorts, A.T. Vessoni, V.M. Victor, M. Vidal, C. Vidoni, O. V. Vieira, R.D. Vierstra, S. Viganó, H. Vihinen, V. Vijayan, M. Vila, M. Vilar, J.M. Villalba, A. Villalobo, B. Villarejo-Zori, F. Villarroya, J. Villarroya, O. Vincent, C. Vindis, C. Viret, M.T. Viscomi, D. Visnjic, I. Vitale, D.J. Vocadlo, O. V. Voitsekhovskaja, C. Volonté, M. Volta, M. Vomero, C. Von Haefen, M.A. Vooijs, W. Voos, L. Vucicevic, R. Wade-Martins, S. Waguri, K.A. Waite, S. Wakatsuki, D.W. Walker, M.J. Walker, S.A. Walker, J. Walter, F.G. Wandosell, B. Wang, C.Y. Wang, C. Wang, C. Wang, C. Wang, C.Y. Wang, D. Wang, F. Wang, F. Wang, F. Wang, G. Wang, H. Wang, H. Wang, H. Wang, H.G. Wang, J. Wang, J. Wang, J. Wang, J. Wang, K. Wang, L. Wang, L. Wang, M.H. Wang, M. Wang, N. Wang, P. Wang, P. Wang, P. Wang, P. Wang, Q.J. Wang, Q. Wang, Q.K. Wang, Q.A. Wang, W.T. Wang, W. Wang, X. Wang, X. Wang, Y. Wang, Y. Wang, Y. Wang, Y.Y. Wang, Y. Wang, Y. Wang, Y. Wang, Y. Wang, Z. Wang, Z. Wang, Z. Wang, G. Warnes, V. Warnsmann, H. Watada, E. Watanabe, M. Watchon, A. Wawrzyńska, T.E. Weaver, G. Wegrzyn, A. M. Wehman, H. Wei, L. Wei, T. Wei, Y. Wei, O.H. Weiergräber, C.C. Weihl, G. Weindl, R. Weiskirchen, A. Wells, R.H. Wen, X. Wen, A. Werner, B. Weykopf, S.P. Wheatley, J.L. Whitton, A.J. Whitworth, K. Wiktorska, M.E. Wildenberg, T. Wileman, S. Wilkinson, D. Willbold, B. Williams, R.S.B. Williams, R.L. Williams, P. R. Williamson, R.A. Wilson, B. Winner, N.J. Winsor, S.S. Witkin, H. Wodrich, U. Woehlbier, T. Wollert, E. Wong, J.H. Wong, R.W. Wong, V.K.W. Wong, W.W.L. Wong, A.G. Wu, C. Wu, J. Wu, J. Wu, K.K. Wu, M. Wu, S.Y. Wu, S. Wu, S.Y. Wu, S. Wu, W.K.K. Wu, X. Wu, X. Wu, Y.W. Wu, Y. Wu, R.J. Xavier, H. Xia, L. Xia, Z. Xia, G. Xiang, J. Xiang, M. Xiang, W. Xiang, B. Xiao, G. Xiao, H. Xiao, H. Tao Xiao, J. Xiao, L. Xiao, S. Xiao, Y. Xiao, B. Xie, C.M. Xie, M. Xie, Y. Xie, Z. Xie, Z. Xie, M. Xilouri, C. Xu, E. Xu, H. Xu, J. Xu, J.R. Xu, L. Xu, W.W. Xu, X. Xu, Y. Xue, S.M.S. Yakhine-Diop, M. Yamaguchi, O. Yamaguchi, A. Yamamoto, S. Yamashina, S. Yan, S.J. Yan, Z. Yan, Y. Yanagi, C. Yang, D.S. Yang, H. Yang, H.T. Yang, H. Yang, J.M. Yang, J. Yang, J. Yang, L. Yang, L. Yang, M. Yang, P.M. Yang, Q. Yang, S. Yang, S. Yang, S.F. Yang, W. Yang, W.Y. Yang, X. Yang, X. Yang, Y. Yang, Y. Yang, H. Yao, S. Yao, X. Yao, Y.G. Yao, Y.M. Yao, T. Yasui, M. Yazdankhah, P.M. Yen, C. Yi, X.M. Yin, Y. Yin, Z. Yin, Z. Yin, M. Ying, Z. Ying, C.K. Yip, S.P.T. Yiu, Y.H. Yoo, K. Yoshida, S.R. Yoshii, T. Yoshimori, B. Yousefi, B. Yu, H. Yu, J. Yu, J. Yu, L. Yu, M.L. Yu, S.W. Yu, V.C. Yu, W.H. Yu, Z. Yu, Z. Yu, J. Yuan, L.Q. Yuan, S. Yuan, S.S.F. Yuan, Y. Yuan, Z. Yuan, J. Yue, Z. Yue, J. Yun, R.L. Yung, D.N. Zacks, G. Zaffagnini, V.O. Zambelli, I. Zanella, Q.S. Zang, S. Zanivan, S. Zappavigna, P. Zaragoza, K.S. Zarbalis, A. Zarebkohan, A. Zarrouk, S.O. Zeitlin, J. Zeng, J. Deng Zeng, E. Žerovnik, L. Zhan, B. Zhang, D.D. Zhang, H. Zhang, H. Zhang, H. Zhang, H. Zhang, H. Zhang, H. Zhang, H.L. Zhang, J. Zhang, J. Zhang, J.P. Zhang, K.Y.B. Zhang, L.W. Zhang, L. Zhang, L. Zhang, L. Zhang, L. Zhang, M. Zhang, P. Zhang, S. Zhang, W. Zhang, X. Zhang, X.W. Zhang, X. Zhang, X. Zhang, X. Zhang, X. Zhang, X.D. Zhang, Y. Zhang, Y. Zhang, Y. Zhang, Y.D. Zhang, Y. Zhang, Y.Y. Zhang, Y. Zhang, Z. Zhang, Z. Zhang, Z. Zhang, Z. Zhang, Z. Zhang, Z. Zhang, H. Zhao, L. Zhao, S. Zhao, T. Zhao, X.F. Zhao, Y. Zhao, Y. Zhao, Y. Zhao, Y. Zhao, G. Zheng, K. Zheng, L. Zheng, S. Zheng, X.L. Zheng, Y. Zheng, Z.G. Zheng, B. Zhivotovsky, Q. Zhong, A. Zhou, B. Zhou, C. Zhou, G. Zhou, H. Zhou, H. Zhou, H. Zhou, J. Zhou, J. Zhou, J. Zhou, K. Zhou, R. Zhou, X.J. Zhou, Y. Zhou, Y. Zhou, Y. Zhou, Z.Y. Zhou, Z. Zhou, B. Zhu, C. Zhu, G.Q. Zhu, H. Zhu, H. Zhu, H. Zhu, W.G. Zhu, Y. Zhu, Y. Zhu, H. Zhuang, X. Zhuang, K. Zientara-Rytter, C.M. Zimmermann, E. Ziviani, T. Zoladek, W.X. Zong, D.B. Zorov, A. Zorzano, W. Zou, Z. Zou, Z. Zou, S. Zuryn, W. Zwerschke, B. Brand-Saberi, X.C. Dong, C.S. Kenchappa, Z. Li, Y. Lin, S. Oshima, Y. Rong, J.C. Sluimer, C.L. Stallings, C.K. Tong, Guidelines for the use and interpretation of assays for monitoring autophagy (4th edition)1, Autophagy. 17 (2021) 1–382. doi:https://doi.org/10.1080/15548627.2020.1797280.

[63] N. Mizushima, T. Yoshimori, How to interpret LC3 immunoblotting, Autophagy 3 (2007) 542–545, https://doi.org/10.4161/AUTO.4600.

[64] M.G. Kearse, J.E. Wilusz, Non-AUG translation: a new start for protein synthesis in eukaryotes, Genes Dev. 31 (2017) 1717–1731, https://doi.org/10.1101/GAD.305250.117.

[65] S.R. Starck, J.C. Tsai, K. Chen, M. Shodiya, L. Wang, K. Yahiro, M. Martins-Green, N. Shastri, P. Walter, Translation from the 5′ untranslated region shapes the integrated stress response, Science 351 (2016), https://doi.org/10.1126/SCIENCE.AAD3867.

[66] A. Sendoel, J.G. Dunn, E.H. Rodriguez, S. Naik, N.C. Gomez, B. Hurwitz, J. Levorse, B.D. Dill, D. Schramek, H. Molina, J.S. Weissman, E. Fuchs, Translation from unconventional 5′ start sites drives tumour initiation, Nature 541 (2017) 494–499, https://doi.org/10.1038/NATURE21036.

[67] O.S. Kwon, S. An, E. Kim, J. Yu, K.Y. Hong, J.S. Lee, S.K. Jang, An mRNA-specific tRNAi carrier eIF2A plays a pivotal role in cell proliferation under stress conditions: stress-resistant translation of c-Src mRNA is mediated by eIF2A, Nucleic Acids Res. 45 (2017) 296–310, https://doi.org/10.1093/NAR/GKW1117.

[68] A.A. Komar, S.R. Gross, D. Barth-Baus, R. Strachan, J.O. Hensold, T.G. Kinzy, W. C. Merrick, Novel characteristics of the biological properties of the yeast Saccharomyces cerevisiae eukaryotic initiation factor 2A, J. Biol. Chem. 280 (2005) 15601–15611, https://doi.org/10.1074/JBC.M413728200.

[69] A. Bretin, J. Carrière, G. Dalmasso, A. Bergougnoux, W. B'chir, A.C. Maurin, S. Müller, F. Seibold, N. Barnich, A. Bruhat, A. Darfeuille-Michaud, H.T.T. Nguyen, Activation of the EIF2AK4-EIF2A/eIF2α-ATF4 pathway triggers autophagy response to Crohn disease-associated adherent-invasive Escherichia coli infection,

Autophagy 12 (2016) 770–783, https://doi.org/10.1080/15548627.2016.1156823.
[70] R. Anderson, A. Agarwal, A. Ghosh, B.J. Guan, J. Casteel, N. Dvorina, W. M. Baldwin, B. Mazumder, T.Y. Nazarko, W.C. Merrick, D.A. Buchner, M. Hatzoglou, R.V. Kondratov, A.A. Komar, eIF2A-knockout mice reveal decreased life span and metabolic syndrome, FASEB J. 35 (2021), https://doi.org/10.1096/FJ.202101105R.
[71] S. Ma, I.Y. Attarwala, X.Q. Xie, SQSTM1/p62: a potential target for neurodegenerative disease, ACS Chem. Nerosci. 10 (2019) 2094–2114, https://doi.org/10.1021/ACSCHEMNEURO.8B00516.